Contents list available at CBIORE journal website

International Journal of Renewable Energy Development

Journal homepage: https://ijred.cbiore.id

Research Article

Unlocking run-of-river hydropower potential in semi-arid regions through modular turbines

Imane El Kasimi*, Moulay Driss Hasnaoui, Driss Khomsi

Hydraulic System Analysis Team (HSAT) Laboratory, Mohammadia School of Engineers, Mohammed V University, Rabat, Morocco

Abstract. The growing global demand for renewable energy has increased the need to diversify electricity systems toward low-impact sources. In this context, run-of-river hydropower plants are increasingly recognized as promising options, as they can generate electricity with relatively limited environmental and social disruption. However, their potential in arid and semi-arid regions remains underexplored, especially under highly variable hydrological conditions. In this context, this study assesses the technical hydropower potential of the semi-arid Bouregreg watershed in Morocco using a distributed run-of-river scheme. The Soil and Water Assessment Tool model was used to simulate streamflow and establish power-duration curves throughout the watershed. These curves were then used to estimate the technical potential based on a modular turbine system consisting of an optimal number of identical Crossflow turbines operating in parallel. The calculations incorporated technical and environmental constraints and were complemented by a preliminary cost assessment. The potential was also evaluated under typical, extreme dry, and extreme wet hydrological conditions. The results indicate a total hydropower potential of 34.3 MW under typical conditions, increasing to 89 MW under wet conditions and decreasing to 12.5 MW under dry conditions. Although the cost analysis revealed values slightly higher than reported average small-hydropower costs, some sites remained within reasonable cost ranges, particularly in the Grou subwatershed, where the estimated annual energy production could potentially cover approximately 58% of its population's annual electricity demand under normal hydrological conditions. These findings highlight the existence of underexploited potential of run-of-river systems in semi-arid basins and provide a preliminary framework for identifying viable hydropower opportunities.

Keywords: Run-of-river, Hydropower, Hydrological modeling, SWAT, Flow-duration curve, Modular turbines, Semi-arid

Received: 7th March 2026; Revised: 28th June 2026; Accepted: 17th July 2026; Available online: 3rd August 2026

1. Introduction

Global electricity demand has been steadily increasing and is expected to continue rising in the coming decades. In 2024, global demand grew by 2.2%, exceeding the average growth rate of 1.3% observed since 2013 (IEA, 2025). This pressure has prompted a global shift toward non-conventional and renewable energy technologies, which has accelerated sharply in recent years (Naidu *et al.*, 2024). It is largely fueled by climate-mitigation policies, declining costs of renewable technologies, and ambitious national energy strategies (Nandnaba, 2025). As a result, for the first time on record, renewable energies surpassed coal in the global electricity mix during the first half of 2025, underscoring their expanding contribution to energy systems (Ember, 2025).

Within the portfolio of renewable energies, hydropower remains the largest contributor to global electricity generation, supplying 14% of global power in 2024 (IHA, 2025). Hydropower is valued for its long lifetime, low operational emissions, cost competitiveness, and flexibility, which is why it is expected to play a central role in future energy transition and climate-mitigation strategies (IRENA, 2025; Sahrakorpi, Khosravi, & Assad, 2021). In fact, global projections indicate that an additional 800 GW of installed hydropower capacity will be required by 2050 to help meet the Sustainable Development Goals and the objectives of the Paris Agreement (IRENA, 2018).

Among the different hydropower technologies, run-of-river (RoR) systems have experienced a notable surge in interest in recent years (Mills-Novoa & Borgias, 2025). These systems generate electricity with little to no storage, relying primarily on instantaneous river flow to produce power (Khan & Pal, 2020). Compared to reservoir-based hydropower plants, RoR schemes generally induce fewer alterations to the natural flow regime and, depending on the plant design, can also result in lower impacts on water quality, fish migration, and aquatic ecosystems (Killingtveit, 2020; Kuriqi *et al.*, 2021). Economically, RoR systems offer several advantages over large-scale hydropower, including lower construction costs and lower labor needs (Maroufpoor & Qin, 2025). In comparison, their land occupation is minimal, and their CO_2 emissions during construction and operation are significantly lower (Huang *et al.*, 2023). In addition, studies report positive public perception of such projects when they provide socioeconomic benefits; in many documented cases, RoR developments have facilitated employment, stimulated local business opportunities, and improved overall quality of life in surrounding communities (UNIDO & ICSHP, 2022). These characteristics make RoR particularly appealing for rural environments, where they can

* Corresponding author
Email: elkasimi@emi.ac.ma (I. El Kasimi)

https://doi.org/10.61435/ijred.2026.62467
ISSN: 2252-4940/© 2026.The Author(s). Published by CBIORE

provide decentralized access to electricity and support sustainable development, especially in developing countries (Malhan & Mittal, 2021).

In order to fully benefit from these advantages, RoR development requires a structured methodology for estimating hydropower potential. The approach generally begins with site selection, the main objective of which is to identify locations with the highest potential for energy generation (International Finance Corporation, 2015). This process relies on the collection and processing of multiple datasets concerning hydrology, topography, and geology from onsite measurements and remote sensing methods (Energy Sector Management Assistance Program, 2021; Golgojan, White, & Bertram, 2025). The data are then analyzed using Geographic Information Systems and hydrological models to evaluate the amount of energy that could be effectively generated at each candidate site (Energy Sector Management Assistance Program, 2021).

At the most simplified level of hydropower assessment, the theoretical potential is calculated under the assumption of ideal conditions, without considering any hydraulic, mechanical, or operational losses (Dhaubanjar *et al.*, 2024). Owing to its simplistic formulation, this type of assessment is widely adopted in hydropower studies, particularly in preliminary evaluations where detailed technical or site-specific data are lacking (Magaju, Cattapan, & Franca, 2020). A more realistic estimation is given by the technical potential, which incorporates physical and technological constraints. This includes the characteristics of the turbine and other equipments of the hydropower plant (Kuriqi *et al.*, 2019; Rumbayan & Rumbayan, 2023). Finally, when economic constraints are introduced by accounting for the costs of construction, operation, and maintenance, the economically feasible potential of hydropower can be determined (Hoes *et al.*, 2017). Compared to the theoretical potential, both the technical and economically feasible potentials provide a more realistic estimate of the energy that can be effectively harnessed from a watershed. However, the economically feasible potential is particularly challenging to evaluate, as it depends on cost and market conditions that fluctuate across time and space (Kumar *et al.*, 2011).

While many studies have assessed the technical and economic feasibility of RoR hydropower, very few have explored its feasibility in regions characterized by arid or semi-arid climates. This lack of attention can be attributed to the strong sensitivity of RoR schemes to flow variability, a defining feature of these climates (Kumar *et al.*, 2011). Moreover, water scarcity is a major concern in arid regions and is expected to intensify under climate change, which has placed hydropower development on the back burner in many African countries (IEA, 2020). In the Middle East and North Africa, studies indicate that increasing the number of dams could further exacerbate water scarcity, making large hydropower development even less appealing (Wheater, 2025).

However, recent evidence shows that hydropower can remain resilient under extreme hydrological conditions. For example, hydropower plants have been able to sustain relatively high outputs even during prolonged drought periods (Fälth *et al.*, 2025). Similarly, in Morocco, previous research identified a theoretical RoR hydropower potential of 32.4 MW in the semi-arid Grou watershed, suggesting that RoR development may remain viable even under water-limited conditions (El Kasimi *et al.*, 2025).

In addition, several design considerations can enhance the feasibility of such plants, particularly the number and configuration of turbines, including whether they are installed in parallel or side-by-side arrangements. Operating multiple turbines, potentially of different sizes or types, in parallel can increase both the energy output of the plant and its economic viability (Anagnostopoulos & Papantonis, 2007). The use of multiple turbines also improves overall plant efficiency by enabling the system to operate closer to its optimal performance across a wider range of discharges (Duncan, 2012). Furthermore, parallel arrangements enhance operational flexibility, allowing electricity production to continue even when one unit is undergoing maintenance (Duncan, 2012). Such flexibility is particularly advantageous under conditions of seasonal flow variability (Anagnostopoulos & Papantonis, 2007; Yildiz, Brown, & Rougé, 2024). This characteristic is especially relevant for RoR schemes, where energy production directly depends on the natural variability of river discharge.

Such results reinforce the need for adapted assessment frameworks that can support the sustainable deployment of RoR systems in arid regions. This gap in the literature is particularly pressing given the growing global interest in RoR technologies. Many countries, such as Costa Rica, Chile, and Ecuador, are directing substantial investments toward RoR projects, and it is projected that approximately 13% of future installed hydropower capacity worldwide will be developed in the form of RoR schemes (IEA, 2021).

Consequently, this study aims to develop a methodology for assessing the technical hydropower potential of semi-arid watersheds using RoR technology. The proposed approach is applied to the Bouregreg watershed in Morocco. First, streamflow across the basin is simulated using the Soil and Water Assessment Tool model. The simulated discharge series are then used to construct flow-duration curves, which are subsequently converted into power-duration curves. Based on these curves, the technical hydropower potential of the watershed is evaluated under median, extreme dry, and extreme wet hydrological conditions. The assessment relies on a modular turbine configuration consisting of several identical turbines arranged in parallel, each operating within its technical limits. Environmental constraints are also incorporated to reduce the potential impacts of the proposed RoR development. Finally, a preliminary cost assessment is conducted to provide an initial evaluation of the economic viability of the proposed configuration.

2. Materials and methods

2.1 Study area

The study area is the Bouregreg watershed, located in northwestern Morocco, with a total surface area of 9545 km². The climate of the basin is classified as Mediterranean with oceanic influences and is characterized by marked seasonal variability. The watershed is structured around three major subwatersheds: Upper Bouregreg (3921 km²), Grou (3776 km²), and Korifla (1848 km²) (Fig. 1). These tributaries converge at the Sidi Mohamed Ben Abdellah dam (SMBA), which is designed exclusively to supply water to some of Morocco's largest urban centers, including Rabat, Casablanca, Mohammedia, and Salé (Agence du Bassin Hydraulique du Bouregreg et de la Chaouia,n.d).

The Upper Bouregreg provides the largest contribution, followed by the Grou and Korifla subwatersheds (Cherrad, 1997). This distribution reflects the spatial precipitation gradient within the watershed, a characteristic of semi-arid climates, with mean annual rainfall of approximately 450 mm in the northwestern downstream areas near the outlet, increasing to about 750 mm in the southeastern upstream regions (Ezzaouini *et al.* 2020).

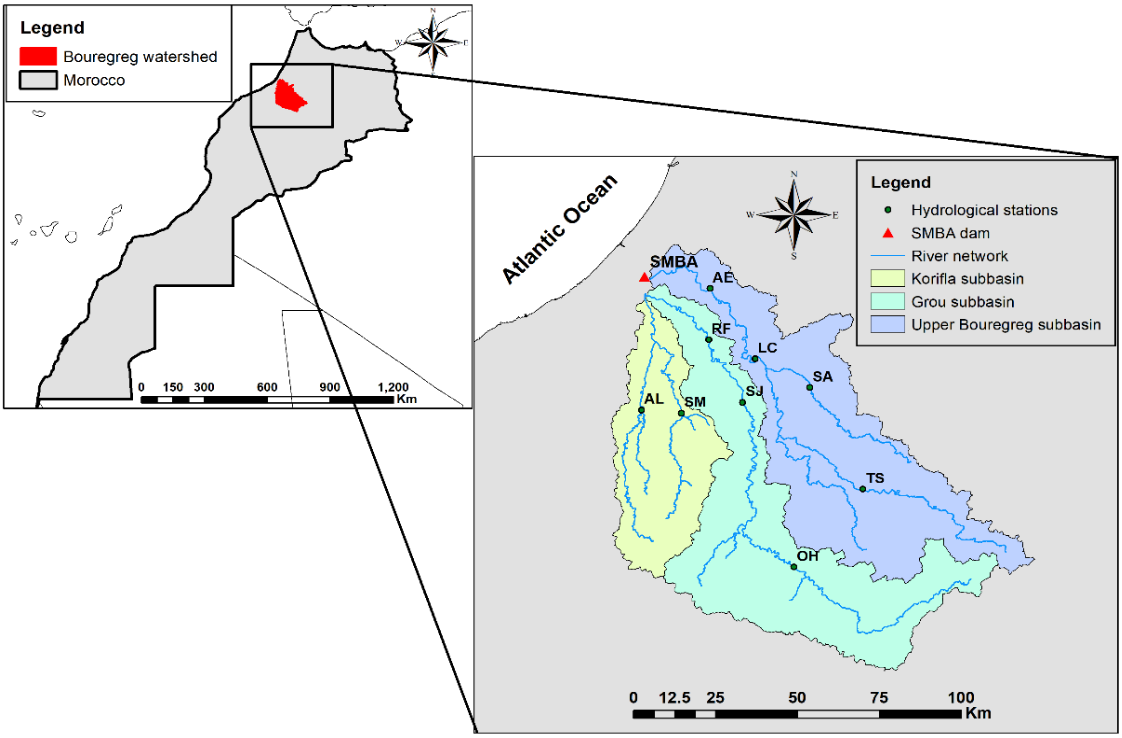

Fig. 1 Location of the Bouregreg watershed (ESRI, 2013)

Rainfall and discharge surveillance within the basin is ensured through a network of hydrological stations. The Upper Bouregreg basin is monitored by four stations — Aguibat Ezziar (AE), Lalla Chafia (LC), Sidi Amar (SA), and Tsalat (TS); the Grou basin by three stations — Ras El Fathia (RF), Sidi Jabeur (SJ), and Ouljet Haboub (OH); and the Korifla basin by two stations — Ain Loudah (AL) and Sidi Mohamed Cherif (SM) (Fig. 1).

2.2 Hydropower potential assessment

The evaluation of hydropower potential aims to estimate the contribution of a power plant, which primarily depends on the hydrologic conditions of the streams and the characteristics of the plant. In particular, the power produced is determined by three key parameters: the net head, the design discharge, and the efficiency of the turbine and generator unit. This potential is typically calculated using the following formula (Kuriqi *et al.*, 2019):

$$P = \eta_g {*} \eta_t {*} \rho {*} g {*} H_{net} {*} Q_d \quad (1)$$

Where P is the hydropower potential (W), η_g is the generator efficiency (%), η_t is the turbine efficiency (%), ρ is the water density (kg/m^3), g is the gravitational acceleration (m/s^2), H_{net} is the net head (m), and Q_d is the design discharge of the turbine (m^3/s).

2.2.1 RoR plant type and site selection

The selected RoR plant configuration influences both the mode of operation and the definition of key design parameters, including weir height, diversion layout, turbine location, and the range of exploitable heads. In this study, a non-diversion RoR scheme is considered, in which hydropower is generated directly at the weir and turbines are installed within or immediately adjacent to the weir structure (Kuriqi *et al.*, 2021; Tsuanyo *et al.*, 2023). This configuration generally results in lower environmental and ecological impacts. Since water is exploited directly at the weir, the natural river regime remains less altered, particularly during low-flow periods, which are often the most sensitive to RoR operations. Moreover, the absence of a depleted river reach downstream of the weir reduces potential impacts on fluvial habitats and water quality. Several studies have reported limited or negligible changes in upstream and downstream biophysical conditions for this type of RoR configuration (Kuriqi *et al.*, 2021).

To assess the potential of a watershed exhaustively, multiple successive RoR plants along the rivers are generally considered (Kusre *et al.*, 2010; A. Pandey, Lalrempuia, & Jain, 2015). However, the spacing between successive plants must be carefully determined before further calculations. The outflow from an upstream plant can significantly affect the hydraulic conditions and pondage of downstream sites, where maintaining relatively stable water levels is essential to prevent operational disturbances (Roy *et al.*, 2022). Furthermore, ensuring sufficient spacing between sites helps reduce the environmental impacts associated with flow alterations induced by hydropower facilities (Joshi & Mishra, 2024). To address this, previous studies have applied minimum buffer distances between sites ranging from 500 m to 3 km (Ayele, 2020; Thin *et al.*, 2020). Building on these considerations, a minimum spacing of 5 km was adopted in the present study.

Additionally, sites located within environmentally or socially sensitive areas were excluded from the assessment, including national parks, hunting reserves, biological and ecological reserves, and densely populated areas. To identify and filter these locations, the Land Use/Land Cover and the protected areas maps were used (Karra *et al.*, 2021; UNEP-WCMC, 2026).

2.2.2 Net Head and design discharge

The net head is obtained by subtracting the total head losses from the gross head. These losses result from water friction along pipes and junctions, turbulence at bends and transitions, and fluctuations in the intake and tailwater levels (Penche, 1998). Ultimately, the accurate calculation of net head requires detailed knowledge of the plant configuration and hydraulic conditions (Martins Da Silva, Camacho, & Ferreira, 2024). In diversion RoR schemes, the available head is often controlled by the topographic difference between the intake and the powerhouse. In contrast, for non-diversion schemes, the gross head is mainly governed by the hydraulic drop created by the weir, which can reach up to approximately 9 m (Sasthav & Oladosu, 2022). Additionally, in preliminary hydropower potential assessments, most studies simplify the analysis by assuming a constant net head (Basso & Botter, 2012). Following this approach, the present study adopts a net head of 5 m created by the weir, representing the average value used in RoR studies (Huang *et al.*, 2023).

The second key factor determining hydropower potential is the design discharge of the turbine. Typically, lower discharges are available over longer durations, thereby ensuring more stable energy generation. However, as shown by Eq. 1, a low discharge results in limited hydropower potential, which is particularly restrictive in semi-arid regions such as the Bouregreg watershed. For this reason, low-discharge designs are usually preferred for rural electrification, isolated communities, and off-grid projects (AHEC, 2013). Conversely, to achieve higher output in grid-connected projects, larger design discharges should be considered (Hänggi & Weingartner, 2012) . For such cases, Tsuanyo *et al.* (2023) suggested using discharges available between 50 and 90 days per year. In alignment with this approach, the present study adopts a more ambitious criterion by selecting the discharge available 30 days per year as the design discharge, to maximize energy generation within the Bouregreg watershed.

Environmental considerations are incorporated by reserving a share of the total discharge as environmental flow. This flow is released downstream without being used for power generation, in order to maintain the quantity and quality of water required for aquatic ecosystems (Arthington *et al.*, 2018). In recent years, increasing attention has been given to the integration of environmental flows into RoR hydropower planning and policy. Their inclusion, however, reduces the volume of water available for energy production, making it necessary to find a balance between ecological preservation and hydropower generation. A study by Kuriqi *et al.* (2019) compared the effects of different environmental flow release strategies on both flow regime alteration and hydropower production. The authors concluded that dynamic environmental flow approaches allow energy production to be maximized while minimizing hydrological disturbance. In particular, the recommended approach considered downstream releases corresponding to 10% to 15% of daily flow. Based on these findings, an environmental flow equal to 10% of the daily discharge is adopted in this study, meaning that only 90% of the daily streamflow is considered available for energy production.

2.2.3 Turbine selection and operating model

The choice of the generator depends primarily on the characteristics of the electrical network to be supplied, including parameters such as frequency, voltage, and the power input delivered by the turbine (Hatata, El-Saadawi, & Saad, 2019). Modern hydro-generators are generally considered highly efficient, with reported performance levels typically ranging between 90% and 97% (ESHA, 2004). In line with these findings, the present study assumes a generator efficiency of 90% for the estimation of the potential.

Hydropower turbines are generally classified into two main categories: impulse turbines and reaction turbines. The key distinction between them lies in their operating principles: impulse turbines convert the kinetic energy of a high-velocity jet of water into mechanical energy, whereas reaction turbines harness the pressure of the water to generate power (Bredeson & Cicilio, 2023). Each type is more suitable for particular hydrological and site conditions. In general, impulse turbines achieve higher efficiency at medium to high heads with relatively low flows, whereas reaction turbines are more efficient under low heads with high flows (Ahmad *et al.*, 2024). Accordingly, the optimal turbine choice for a given project is determined primarily by the ranges of net head and design discharge available at the site. In practice, reaction turbines such as Kaplan and Francis dominate in large-scale hydropower projects, as their higher costs and technical complexity are feasible in large installations (U.S. Department of Energy, n.d.). By contrast, impulse turbines combine mechanical simplicity with low manufacturing and maintenance demands, resulting in lower costs and larger use in small hydropower and rural electrification schemes (Bragalli, Micocci, & Naldi, 2023; B. Pandey & Karki, 2016). The cost advantage becomes especially relevant in low-head schemes where electromechanical equipment expenses can represent nearly 40% of the total capital cost (IEA, 2021). They also maintain relatively consistent efficiency over a wide range of discharges (Yildiz & Vrugt, 2019).

Among impulse turbines, the Crossflow turbine has gained particular attention because of its compact dimensions, ease of manufacture, and stable efficiency performance typically ranging from 70% to 85% (Adhikari & Wood, 2018). While its efficiency is slightly lower compared to other turbines, its performance curve is notably flat; in other words, when discharges drop significantly below the design discharge, efficiency remains relatively unchanged rather than decreasing sharply (Hatata, El-Saadawi, & Saad, 2019). This feature is especially advantageous for RoR plants, which are highly vulnerable to variable flow conditions, and explains why Crossflow turbines are widely used in such schemes (Hatata, El-Saadawi, & Saad, 2019). Although impulse turbines are conventionally associated with higher heads, several experimental and numerical studies have evaluated the performance of Crossflow turbines at very low heads, even as low as 1.17 m, and still reported efficiencies approaching 91% (Mehr *et al.*, 2021). Accordingly, this turbine type is adopted in the present study to estimate the potential of the proposed RoR scheme.

Like other turbines, the Crossflow turbine operates within a restricted discharge range, defined by a minimum and maximum flow capacities. The minimum discharge is usually expressed as a fraction of the design discharge; for Crossflow turbines, this is reported as 15% of the design discharge (Penche, 1998). At the upper limit, Crossflow turbines can typically accommodate a maximum discharge of 10 m^3/s (Kadier *et al.*, 2018). To ensure safe plant operation, an additional margin is sometimes applied to account for extreme flow or flood events (Hänggi & Weingartner, 2012). Consequently, the performance of the turbine follows the approach described by Yildiz & Vrugt (2019):

Table 1
Summary of technical and environmental considerations for RoR potential assessment

Parameter	Specification
Net head	5 m
Design discharge	90 % of $Q_{30\ days}$
Turbine type	Crossflow
Maximum flow	10 m^3/s
Minimum flow	15 % of $Q_{30\ days}$
Safety flow	$Q_{7\ days}$
Environmental flow	10 % of the daily discharge
Turbine efficiency	Eq. 3
Generator efficiency	90 %
Sites spacing	5 km
Excluded sites	Densely populated areas and environmentally protected areas.

$$Q(t) = \begin{cases} 0 \text{ if } Q \leq Q_{min} \\ Q \text{ if } Q_{min} < Q \leq Q_{max} \\ Q_{max} \text{ if } Q_{max} < Q \leq Q_{safety} \\ 0 \text{ if } Q > Q_{safety} \end{cases} \quad (2)$$

Where Q is the instantaneous discharge admitted by the turbine (m^3/s), Q_{min} is the minimum flow level (m^3/s), Q_{max} is the maximum flow level (m^3/s), Q_{safety} is the safety threshold flow level (m^3/s). Following Yildiz & Vrugt (2019), Q_{safety} is defined as the discharge corresponding to a 2% exceedance probability

Finally, the turbine efficiency depends on its characteristics. Formulas have been established through experimental studies to precisely determine the efficiency of each type of turbine. In the case of the Crossflow turbine, the formula is relatively simple and depends only on the discharge flowing through the turbine and the design discharge, as expressed in the following equation (Minister of Natural Resources Canada, 2004):

$$\eta_t = 0.79\text{-}0.15*\frac{Q_d\text{-}Q}{Q_p}\text{-}1.37*(\frac{Q_d\text{-}Q}{Q_p})^{14} \quad (3)$$

Where η_t is the turbine efficiency, Q is the instantaneous discharge admitted by the turbine (m3/s), Q_d is the design discharge (m^3/s), Q_p is the peak efficiency flow (m^3/s), which in the case of the Crossflow turbine, is defined as the design discharge Q_d (Minister of Natural Resources Canada, 2004).

In summary, Table 1 presents a summary of the technical and environmental considerations adopted in this study for the assessment of RoR potential.

2.3 Hydrological modeling and FDC development

2.3.1 SWAT model setup

Once potential sites are identified, the subsequent step is to evaluate the discharge available at each location, which can be achieved through hydrological modeling. Among the existing models, the Soil and Water Assessment Tool (SWAT) is one of the most widely applied in hydropower studies. Its applications encompass a broad spectrum of hydropower assessment contexts, ranging from large-scale evaluations coupled with climate change projections to studies in water-scarce basins (Garcia *et al.*, 2024; Marcinkowski, 2025).

The SWAT model simulates a range of watershed processes, including hydrology, sediment transport, pollutant dynamics, crop growth, and land management practices. The basin is first delineated into sub-basins, which are subsequently divided into hydrologic response units (HRUs). Each HRU corresponds to a unique combination of land use, soil type, and topographic features. The outputs of the water balance equation for individual HRUs are then combined to represent the overall hydrological response of the subbasin (Arnold *et al.*, 2012). To enable this representation, the model requires the integration of both spatial and hydrometeorological input data. The essential spatial layers include a Digital Elevation Model (DEM), a Land Use/Land Cover map (LULC), and a soil map, which together define the watershed's physical and surface characteristics. In parallel, daily hydrometeorological inputs are needed, including precipitation, maximum and minimum air temperature, relative humidity, solar radiation, and wind speed (Arnold *et al.*, 2012).

For this study, daily rainfall data were obtained from the nine hydrological stations distributed across the watershed (Fig. 1), covering the period 1983–2020. The remaining climatic variables were extracted from the ERA5-Land reanalysis database (Copernicus Climate Change Service, 2019). Spatial input layers included a 12.5 m resolution DEM derived from ALOS PALSAR, a 10 m resolution LULC map generated from Sentinel-2 imagery, and soil characteristics obtained from the FAO soil map (ASF DAAC, 2014; Karra *et al.*, 2021; FAO, 1971).

2.3.2 Calibration and validation

The input data described above were used to construct an initial SWAT model of daily runoff for the period 1983–2020. The simulated runoff must then be compared with the observed discharge data from the nine hydrometric stations located within the watershed. This constitutes the calibration step, during which the model parameters governing runoff generation are adjusted until the simulated and observed hydrographs match as closely as possible (Shen, Tolson, & Mai, 2022). A validation step is needed eventually to test the calibrated model on another independent set of observed data and to confirm the validity of the calibrated parameters (Biondi *et al.*, 2012).

To perform these steps, the SWAT Calibration and Uncertainty Procedures software (SWAT-CUP) is commonly used. It offers several calibration algorithms, out of which the Sequential Uncertainty Fitting version 2 (SUFI-2) is the most frequently applied. It effectively determines optimal parameter ranges while minimizing computational cost for complex hydrological processes (Wu & Chen, 2015). The algorithm operates by optimizing an objective function such as the coefficient of determination, the Nash–Sutcliffe efficiency (NSE), and Kling–Gupta efficiency (Abbaspour, 2015).

The performance of both calibration and validation processes is generally assessed using statistical performance

Table 2
SWAT performance metrics for daily runoff *(Kadier et al., 2018)*

Performance	NSE	PBIAS
Very Good	NSE≥0.7	|PBIAS|≤0.25
Good	0.5≤NSE<0.7	0.25<|PBIAS|≤0.5
Satisfactory	0.3≤NSE<0.5	0.5<|PBIAS|≤0.7
Unsatisfactory	NSE<0.3	|PBIAS|>0.7

indicators, among which the NSE and the Percent Bias (PBIAS) are the most widely used. Their formulations are presented in Equations (4) and (5), and the corresponding performance thresholds for daily runoff simulations are summarized in Table 2 (Moriasi *et al.*, 2015).

$$NSE = 1-\frac{\sum_{i=1}^{n}(O_i-P_i)^2}{\sum_{i=1}^{n}(O_i-\bar{O})^2} \quad (4)$$

$$PBIAS = \frac{\sum_{i=1}^{n}(O_i-P_i)}{\sum_{i=1}^{n}O_i}*100 \quad (5)$$

Where O_i is the measured discharge (m^3/s), P_i is the simulated discharge (m^3/s), $\bar{O}$ is the mean of measured discharges (m^3/s), and n is the total number of measured discharges.

In this study, the calibration and validation procedures were performed separately for the three main subwatersheds, with the NSE adopted as the objective function in the SUFI-2 algorithm. Runoff measurements were available from the nine hydrometric stations across the study area for the period 1983–2020, except in the Korifla subwatershed, where data were only available until 2016.

Before the calibration process, a five-year period was used to warm up the model, which helps adjust the initial conditions of the SWAT model to more realistic and stable values (Kim, Kwon, & Han, 2018). As for the choice of the calibration and validation periods, there is no strict general rule; however, several considerations must be respected to ensure an effective and efficient calibration process (Shen, Tolson, & Mai, 2022). The simplest method, as suggested by Li *et al.* (2012), recommends that both periods be hydrologically similar, representing a similar range of climatic and flow conditions, such as wet, dry, and average years, in order to avoid bias toward one period. Therefore, the calibration–validation split was defined so that the mean and standard deviation of annual runoff were approximately similar before and after the selected year. Accordingly, a cutoff year of 2010 was adopted for the Korifla and Upper Bouregreg subwatersheds, while 2009 was selected for the Grou subwatershed.

2.3.3 Flow-duration curve construction

Once the daily discharges at the potential sites are simulated through the calibrated and validated SWAT model, the next step is to construct the flow-duration curve (FDC). This graph represents the relationship between river discharge and the number of days per year for which a given discharge is equaled or exceeded (Vogel & Fennessey, 1994). Among its multiple applications, the FDC is widely used in hydropower studies as a basis for turbine sizing and the estimation of energy output from a power plant (Paschetto, Caselle, & Bonetto, 2025).

The FDCs are commonly constructed using quantile estimators that relate discharge values to exceedance probabilities, typically by ranking daily flows and applying a plotting position formula such as the Weibull estimator (Ridolfi, Kumar, & Bárdossy, 2020). However, such simple quantile estimators are highly sensitive to individual order statistics. To address this, more robust estimators based on weighted combinations of multiple order statistics, such as the Harrell–Davis estimator (HD), are often used, as they provide more reliable and efficient quantile estimates (Harrell & Davis, 1982; Akinshin, 2024).

When the FDC is constructed using the entire period of observations, it is referred to as a period-of-record FDC. This plot represents long-term flow regimes, but is highly sensitive to extreme wet and dry years (Vogel & Fennessey, 1994). To overcome this limitation, the annual flow duration curve (AFDC), proposed by Vogel and Fennessey (1994), is preferred, as it represents the interannual variability of flow. It is particularly well-suited for hydropower applications, providing a more realistic estimate of expected site performance while accounting for interannual variability (Ghotbi *et al.*, 2020).

The annual interpretation of FDCs proposed by Vogel and Fennessey (1994) enables the frequency analysis of AFDCs. Suppose that *n* years of observations are available at a given site. Using a quantile estimator, *n* AFDCs can be constructed, one for each year of record. For a given exceedance probability *p*, these annual curves yield *n* streamflow quantile estimates, denoted $Q_1(p)$, $Q_2(p)$,…, $Q_n(p)$, which together form a sample of annual quantiles corresponding to that exceedance level. Vogel and Fennessey (1994) interpret this sample as reflecting interannual hydrological variability, with its lower and upper values corresponding to relatively dry and wet annual conditions, respectively.

More specifically, for each exceedance level *p*, Vogel and Fennessey (1994) define ε as the annual probability of exceedance for high-flow conditions and ν as the annual probability of non-exceedance for low-flow conditions, with $\varepsilon = 1-\nu$. This allows the definition of an annual FDC associated with a specified average recurrence interval *T*, where $T = 1/\varepsilon$ for high flows and $T = 1/\nu$ for low flows. A *T*-year FDC is therefore a hypothetical AFDC that is exceeded, on average, once every *T* years in the case of high flows, or not exceeded, on average, once every *T* years in the case of low flows. Consequently, for each return period *T*, two generalized AFDCs can be derived from the multiple AFDC constructed: a probabilistic wet FDC and a probabilistic dry FDC.

For this study, the AFDCs were established at each potential RoR site using the SWAT-simulated discharge and the HD estimator. Based on these curves, the hydropower assessment at each RoR site was conducted in two steps. First, the historical median hydropower potential was evaluated. For this purpose, the historical median hydrological year was identified for each watershed using the SWAT-simulated annual runoff series at the watershed outlets. The AFDCs corresponding to this median year, hereafter referred to as the median AFDCs, were then used to estimate the hydropower potential at each RoR site. This step provides an assessment of the typical hydropower potential during the simulation period, which is referred to in this study as the historical median scenario. Second, the probabilistic hydropower potential was assessed for selected return periods. AFDCs associated with return periods of 5, 10, and 20 years were constructed using the HD estimator and then used to estimate the corresponding hydropower potentials. This step allowed the evaluation of RoR hydropower performance under hydrological conditions with different frequencies of occurrence. In the following sections, extreme wet and dry scenarios associated with a return period *T* are referred to as Wet (T) and Dry (T).

2.4 Energy Assessment

2.4.1 Annual energy estimation

The yearly energy output of a RoR plant refers to the total amount of electricity generated over a year. It can be expressed by the general equation (Bragalli, Micocci, & Naldi, 2023):

$$E = \frac{1}{1000}\sum_{i=1}^{n} 24*\rho*g*Q_i*H_{net}*\eta_g*\eta_t(Q_i) \quad (6)$$

Where E is the annual energy produced by the plant (Wh), Q_i is the daily flow corresponding to the i-th day on the FDC (m^3/s), ρ is the water density (kg/m^3), g is the gravitational acceleration (m/s^2), H_{net} is the net head (m), η_g is the generator efficiency (%), $\eta_t(Q_i)$ is the turbine efficiency corresponding to the discharge Q_i, and n is the number of days in a year.

In hydropower applications, the energy can also be derived from the power–duration curve (PDC), which indicates the number of days that a given power is available (Schroeder *et al.*, 2023). To build this curve, the discharge availability is first obtained from the FDC. Using Eq. 1, the discharge values are converted into power, and the resulting power values are plotted against their corresponding durations of exceedance, producing a curve that follows the general shape of the FDC. Consequently, Eq. 6 indicates that the yearly energy production corresponds to the area under the PDC.

It is important to note, however, that energy cannot be generated for the entire range of discharges represented by the FDC. As reflected by Eq. 2, turbines operate only within a specific operational range, bounded by a minimum discharge (Q_{min}), a maximum discharge (Q_{max}), and a safety discharge (Qs_{afety}). This restriction ensures efficient hydropower production while protecting the plant and the turbine against excessive flows. Consequently, the technically feasible energy output corresponds only to the portion of the PDC within this operational range, as illustrated in Fig. 2.

2.4.2 Modular turbine configuration

To optimize the energy production at each site, it is desirable to exploit as wide a range of discharges as possible. However, as shown in Fig. 2, a single turbine can operate only within a limited discharge range, which restricts the total amount of energy produced. Moreover, turbine efficiency decreases when the flow deviates from the design discharge (Kumar *et al.*, 2011). Consequently, the use of a single turbine scheme often leaves part of the available flow either underexploited or entirely unused.

To address this limitation, the present study introduces the concept of modular turbines, defined as a set of multiple identical turbines operating in a parallel arrangement. The main objective of this configuration is twofold: (i) to expand the range of discharges that can be harnessed for hydropower production, and (ii) to maximize the number of turbines operating at, or close to, their design efficiency.

At a given site, the proposed configuration consists of *n* identical Crossflow turbines operating in parallel. The total design discharge of the plant is defined as 90% of $Q_{30\ days}$. Accordingly, the design discharge assigned to each turbine is expressed as:

$$Q_d = \frac{0.9\ Q_{30\ days}}{n} \quad (7)$$

Where Q_d is the design discharge of each turbine (m^3/s) and $Q_{30\ days}$ is the discharge exceeded or equaled for 30 days, selected from the AFDC (m^3/s).

Consequently, when operating in a parallel configuration, *i* turbines can accommodate a total discharge given by:

$$Q_i = i*Q_d \quad (8)$$

Where: Q_i is the total discharge admitted by the *i* turbines operating in parallel (m^3/s), *i* is the number of turbines in operation ($1 \le i \le n$), Q_d is the design discharge of each turbine (m^3/s). Let t_i be the exceedance duration associated with the discharge Q_i in the AFDC.

For discharges equal to or greater than Q_n, all turbines operate simultaneously at their design flow, achieving maximum efficiency. However, the n turbines can admit a total discharge of only Q_n; any excess flow beyond this threshold is released without energy conversion, as it exceeds the maximum discharge of the turbine. Consequently, the corresponding

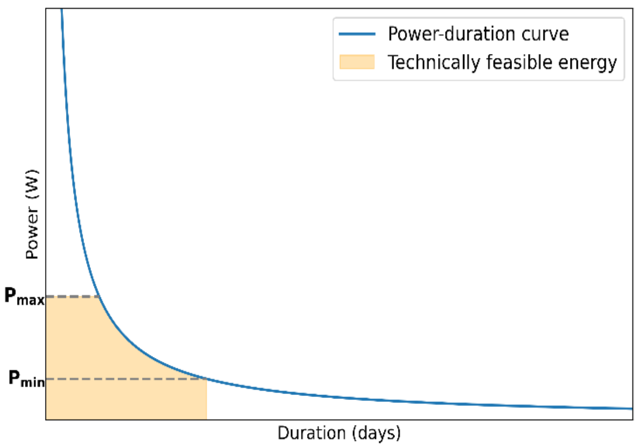

Fig. 2 Technically feasible energy by a single turbine: The powers P_{min} and P_{max} are associated with the discharges Q_{min} and Q_{max} as calculated using Eq. 1

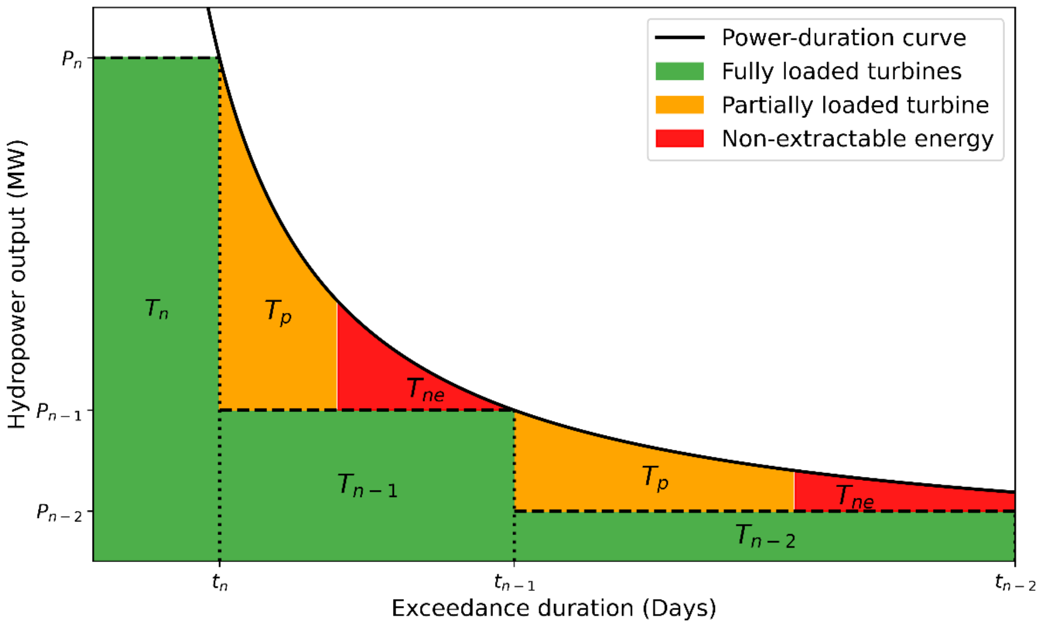

Fig. 3 Conceptual representation of the modular turbine operation on a PDC. P_n, P_{n-1}, and P_{n-2} correspond to the total power produced by n, n-1, and n-2 fully loaded turbines, respectively, while t_n, t_{n-1}, and t_{n-2} represent their corresponding exceedance durations on the PDC. The green areas, T_n, T_{n-1}, and T_{n-2} represent the energy produced by fully loaded turbines. The orange areas, T_p, correspond to the energy produced by one turbine operating under partial-load conditions, while the red areas, T_{ne}, represent non-extractable energy associated with discharge ranges that fall outside the admissible operating limits of the turbines.

technically feasible energy output is represented in Fig. 3 by the area T_n, extending to the duration t_n.

When the available discharge lies between Q_{n-1} and Q_n, only *n-1* turbines are fully loaded, while the remaining turbine processes the residual flow. Since this residual discharge is necessarily lower than Q_d, the turbine operates under partial-load conditions, resulting in a reduced efficiency, as described by Eq. 3. Consequently, the T_{n-1} area in Fig. 3 represents the energy produced by the fully loaded *n-1* turbines, extending to the duration t_{n-1}, while the orange area T_p corresponds to the energy generated by the partially loaded turbine. However, partial load operation is limited: once the residual discharge falls below the minimum operating threshold Q_{min}, energy conversion is no longer possible by the identical turbines. The red area T_{ne} in Fig. 3, therefore, represents non-extractable energy, corresponding to discharges that must be released without energy production.

The same logic applies recursively across the PDC; as discharge decreases, fewer turbines operate at full efficiency, while a single identical turbine handles the remaining flow. This distribution ensures that the majority of turbines continue to operate at or near their maximum efficiency, while only one turbine at any given time functions under partial efficiency. Eventually, for each potential site, the annual energy output is obtained by integrating the area under the PDC, excluding the non-extractable energy areas (Fig. 3).

Given that *n* turbines are considered, an optimization procedure was implemented to maximize the energy production potential. A Python-based algorithm was developed to evaluate the annual energy output of modular configurations comprising between 2 and 10 turbines. For each site, the number of turbines that yields the highest annual energy production is identified and subsequently adopted for the estimation of the hydropower potential of the Bouregreg watershed.

2.4.3 Hydrological uncertainty propagation to hydropower potential

The hydropower estimates depend on the accuracy of the SWAT-simulated discharge series. In fact, the SUFI-2 algorithm enables uncertainty analysis of the SWAT model by accounting for uncertainties related to model inputs, model structure, and parameter values (Khaleghi & Hosseini, 2024). In SUFI-2, uncertainty is represented by the 95% prediction uncertainty (95PPU), which is bounded by the 2.5th and 97.5th percentiles of the cumulative distribution of the simulated runoff obtained through Latin hypercube sampling (Abbaspour, 2015).

Consequently, this uncertainty band was propagated from the simulated discharge series to the hydropower potential calculations. To assess this effect, the optimal number of turbines obtained under the historical median scenario was retained for each station. Then, for each station, the SUFI-2 simulations from the calibrated and validated SWAT model were considered. For each simulation, the corresponding median hydrological year was extracted, and the hydropower potential was then calculated using the same predefined technical and environmental constraints as in the main assessment. Finally, for each station, the hydropower potential values obtained from the simulation ensemble were ranked, and the 2.5th and 97.5th percentiles were used to define the lower and upper limits of the 95PPU of hydropower potential.

2.5 Preliminary economic potential estimation

Only a fraction of the technical hydropower potential can be considered economically exploitable. This fraction is commonly referred to as the economic potential and is generally assessed through the cost of the electricity generated by the plant (Gernaat et al., 2017). This cost includes capital expenditures associated with project development, such as civil engineering works, electromechanical equipment, and grid connection (Wagner & Mathur, 2011). These components typically account for approximately 30%, 40%, and 10%, respectively, of the total installation cost of RoR plants (IEA, 2021). The remaining share is allocated to planning, project development, environmental assessments, permitting procedures, land acquisition, and social and environmental compliance costs (IEA, 2021).

In this study, the preliminary economic assessment was based on the levelized cost of electricity (LCOE), which represents the discounted cost of producing one unit of electricity over the lifetime of the project. The LCOE was calculated for the historical median scenario as follows (Tefera & Kasiviswanathan, 2022):

$$LCOE = \frac{I_{cost} + \sum_{t=1}^{T} \frac{OM_{cost}(1+g)^{t-1} + F}{(1+r)^t}}{\sum_{t=1}^{T} \frac{E}{(1+r)^t}} \quad (9)$$

Where I_{cost} is the initial investment cost, OM_{cost} is the operation and maintenance cost, g is the annual escalation rate of operation and maintenance costs, r is the discount rate, F is the fuel expenditure, E is the annual energy production of the RoR plant (kWh), and T is the project lifetime in years.

The initial investment cost refers to the total direct and indirect expenses required to develop the hydropower project, from civil works and equipment to engineering, mitigation measures, and construction-period interest (Tefera & Kasiviswanathan, 2022). These costs can be estimated using the empirical cost equations provided by RETScreen for small hydropower projects (Minister of Natural Resources Canada, 2004). In the present study, the major components, including civil works, engineering, turbine cost, and generator cost, were first calculated and then grouped as follows:

$$C_{major\ cost} = C_{civil\ works} + C_{engineering} + C_{turbines} + C_{generator} \quad (10)$$

Where $C_{civil\ works}$, $C_{engineering}$, $C_{turbines}$, and $C_{generator}$ are the estimated costs of civil works, engineering, turbine equipment, and generator equipment, respectively.

The remaining indirect and miscellaneous costs were approximated as 13% of the major cost components, following a previous RoR cost assessment study (Singal, Saini, & Raghuvanshi, 2010). Therefore, the total initial investment cost was estimated as:

$$I_{cost} = 1.13 * C_{major\ cost} \quad (11)$$

The operation and maintenance costs are typically estimated as a fixed percentage of the initial investment cost. Based on reported hydropower cost ranges and previous LCOE optimization studies, a rate of 2.5% was adopted (Amougou et al., 2022; IRENA, 2025). Consequently, the operation and maintenance costs were calculated as follows:

$$OM_{cost} = 0.025 * I_{cost} \quad (12)$$

Where OM_{cost} is the operation and maintenance cost, and I_{cost} is the initial investment cost.

Consistent with previous studies, a discount rate of 4% and an annual operation and maintenance cost escalation rate of 2% were adopted, while fuel expenditures were neglected (Golgojan, White, & Bertram, 2025; Tefera & Kasiviswanathan, 2022). A project lifetime of 50 years was adopted, which is consistent with the lifetime generally reported for RoR projects (Amougou et al., 2022; Verán-Leigh & Vázquez-Rowe, 2019).

Since the RETScreen cost equations provide costs in Canadian dollars, all estimated costs were converted to United States dollars (USD) using a conversion factor of 0.72, corresponding to the exchange rate adopted at the time of the analysis (Bank of Canada, n.d.).

It should be noted that this economic assessment provides only a preliminary estimate of the LCOE, as hydropower costs are highly site-specific (Klein & Fox, 2022). Therefore, the resulting LCOE values should be interpreted as screening-level indicators rather than detailed project feasibility estimates. However, in order to compare the obtained results with the statistics reported by IRENA for small hydropower generation costs in 2024, a capacity-weighted average LCOE was calculated for each watershed using the installed capacities of the RoR plants (IRENA, 2025):

$$LCOE_{average} = \frac{\sum_{i=1}^{n} LCOE_i * Cap_i}{\sum_{i=1}^{n} Cap_i} \quad (13)$$

Where $LCOE_i$ is the calculated LCOE indicator for plant *i* (USD/kWh), Cap_i is the capacity of plant *i* (MWh) and n is the number of plants within the considered watershed.

3. Results and discussion

3.1 Model calibration and validation

The resulting daily simulated and observed hydrographs during the calibration and validation periods at the most downstream stations are presented in Fig. 4, and the model's performance across all stations is summarized in Table 3. Overall, the SWAT

Table 3
SWAT model calibration and validation performance across subwatersheds

Subwatershed	Station	Calibration		Validation	
		NSE	PBIAS	NSE	PBIAS
Upper Bouregreg	AE	0.54	-20.4	0.45	-13.2
	LC	0.58	-44.3	0.43	-47.7
	SA	0.31	-23.1	0.45	-21.1
	TS	0.5	16.9	0.38	-20.6
Grou	RF	0.42	-31.2	0.34	-33.9
	SJ	0.39	-36.8	0.31	-39.2
	OH	0.22	22.8	0.22	11.1
Korifla	AL	0.54	-33.9	0.49	-25.8
	SM	0.48	-5.1	0.42	-1.0

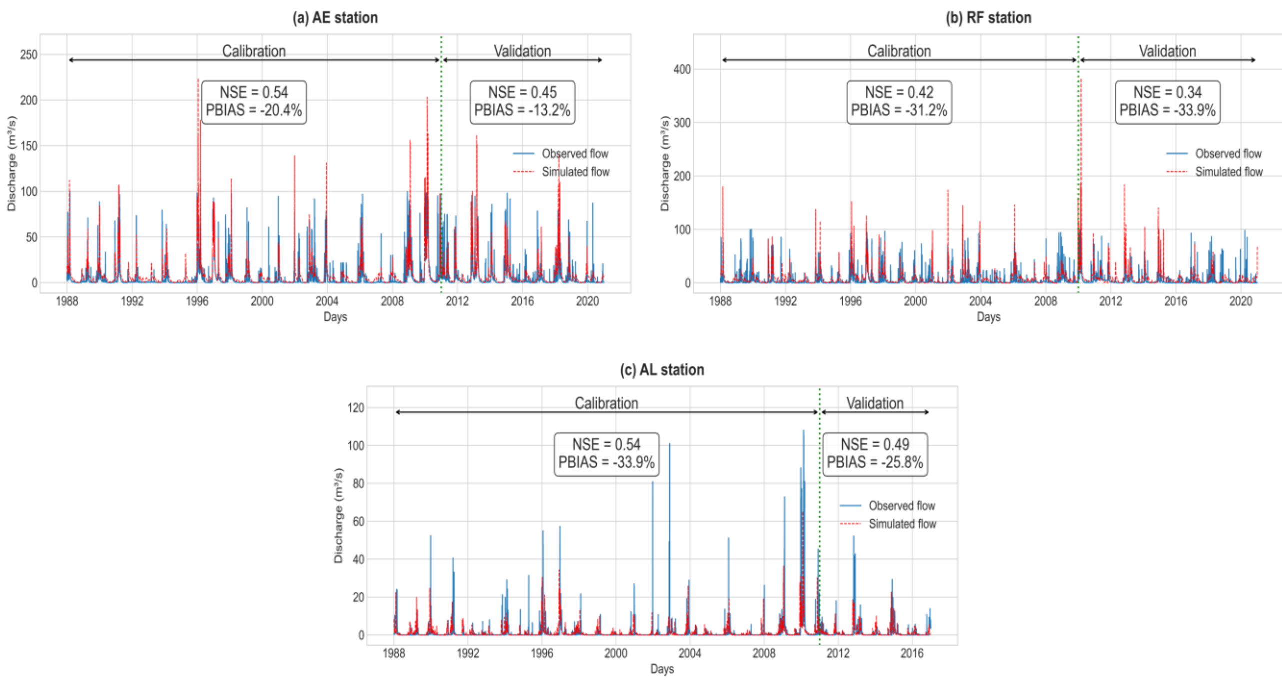

Fig. 4 Observed and simulated hydrographs at: (a) AE station in th Upper Bouregreg watershed, (b) RF station in Grou watershed, (c) AL station in Korifla watershed

model achieved performance levels ranging from satisfactory to good. Among the modeled basins, the most satisfactory performance was obtained for the Korifla and the Upper Bouregreg subwatershed, whereas the Grou subwatershed exhibited the weakest performance, particularly at the OH station. This can be attributed to the fact that OH is the most upstream and spatially isolated station in the Grou subwatershed, as shown in Fig. 1, which makes it more difficult for the model to accurately reproduce local hydrological responses.

The relatively higher performance in the Upper Bouregreg subwatershed can be attributed to the well-distributed network of gauging stations, which allows for more spatially consistent calibration. In contrast, the Korifla subwatershed benefited from its small spatial scale, which enhanced model responsiveness and resulted in stronger calibration and validation statistics despite the shorter period of observed runoff than the other basins. Globally, the model tends to underestimate runoff, as indicated by the predominantly negative PBIAS value.

Nevertheless, the magnitudes of these biases remain within the range of satisfactory performance for both calibration and validation periods. Taken together, the NSE and PBIAS values confirm that the hydrological model provides a reliable representation of the runoff dynamics across the entire Bouregreg watershed.

3.2 Construction and quality of AFDCs

Building upon this calibrated model, the next step is the construction of the FDCs. For an accurate hydropower evaluation, it is essential that FDCs derived from simulated discharges closely match those constructed from observed data. Fig. 5 illustrates the distribution of NSE_{FDC} values obtained from the comparison between observed and simulated FDCs for each hydrological year between 1988 and 2020, across the nine gauging stations. The NSE_{FDC} values ranged from –0.09 to 0.97, with median values between 0.33 and 0.67. Consistent with the calibration and validation results, the most satisfactory FDCs

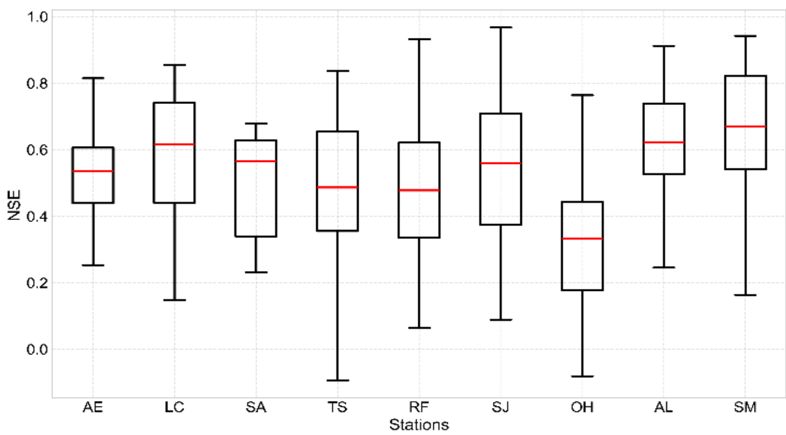

Fig. 5 Range of NSE_{FDC} values across the hydrological stations (Red markers indicate median values)

correspond to the Korifla basin, followed by the Upper Bouregreg basin, while the Grou basin exhibited comparatively lower accuracy. In particular, the OH station stands out as the lowest performing compared to the rest.

To identify the representative median year for each watershed, the total simulated annual runoff values at the corresponding outlet were ranked in ascending order. Based on this ranking, the hydrological years 1988/1989, 2010/2011, and 1993/1994 were identified as the median years for the Upper Bouregreg, Grou, and Korifla subwatersheds, respectively. To further assess the reliability of the simulation, the observed and simulated AFDCs were compared at the gauging stations using the NSE_{FDC} statistic, and the results are presented in Table 4. According to Castellarin *et al.* (2004), NSE_{FDC} values higher than 0.5 are considered satisfactory. Therefore, the model performance can be regarded as satisfactory across all stations except at the OH station, where the NSE_{FDC} value falls below this threshold, likely due to the lower quality of the hydrological simulation at this site. Overall, the AFDC comparison indicates that the model provides an acceptable representation of the flow-duration behaviour at most evaluated stations. However, because hydropower estimates are particularly sensitive to the shape of the FDC, the effect of these deviations on plant design power is further examined in Section 3.3.2 as part of the hydrological uncertainty analysis.

Based on all the AFDCs for each site, probabilistic AFDCs are established using the HD estimator. The probabilistic AFDCs obtained for return periods of 5 and 20 years, along with the median AFDC at the three watershed outlets, are shown in Fig. 6. By construction, as the return period increases, the wet AFDC shifts upward while the dry AFDC shifts downward, which increases the separation between the two curves. This reflects the fact that larger return periods correspond to more extreme interannual conditions, whether wetter or drier. At the watershed scale, the probabilistic AFDCs reveal contrasted interannual flow regimes. The Grou subwatershed exhibits the most stable behavior, with relatively limited variability over a large part of the year, particularly in the medium-flow range, while greater differences appear mainly in the low-flow domain. The Upper Bouregreg subwatershed shows an intermediate level of variability. In contrast, the Korifla subwatershed displays stronger interannual variability across most exceedance probabilities, indicating a higher sensitivity of its flow regime to hydrological conditions.

The AFDC shapes remain broadly similar across return periods for the Upper Bouregreg and Grou subwatersheds, suggesting that interannual variability mainly affects discharge magnitude rather than the overall ranked-flow structure. However, the Grou subwatershed shows a marked break in the terminal low-flow tail under dry conditions, indicating a rapid decline once low-flow support is depleted. Korifla presents a distinctive low-flow plateau in the median and dry AFDCs, followed by a sharp decline toward more severe depletion conditions. This plateau becomes less pronounced under wet

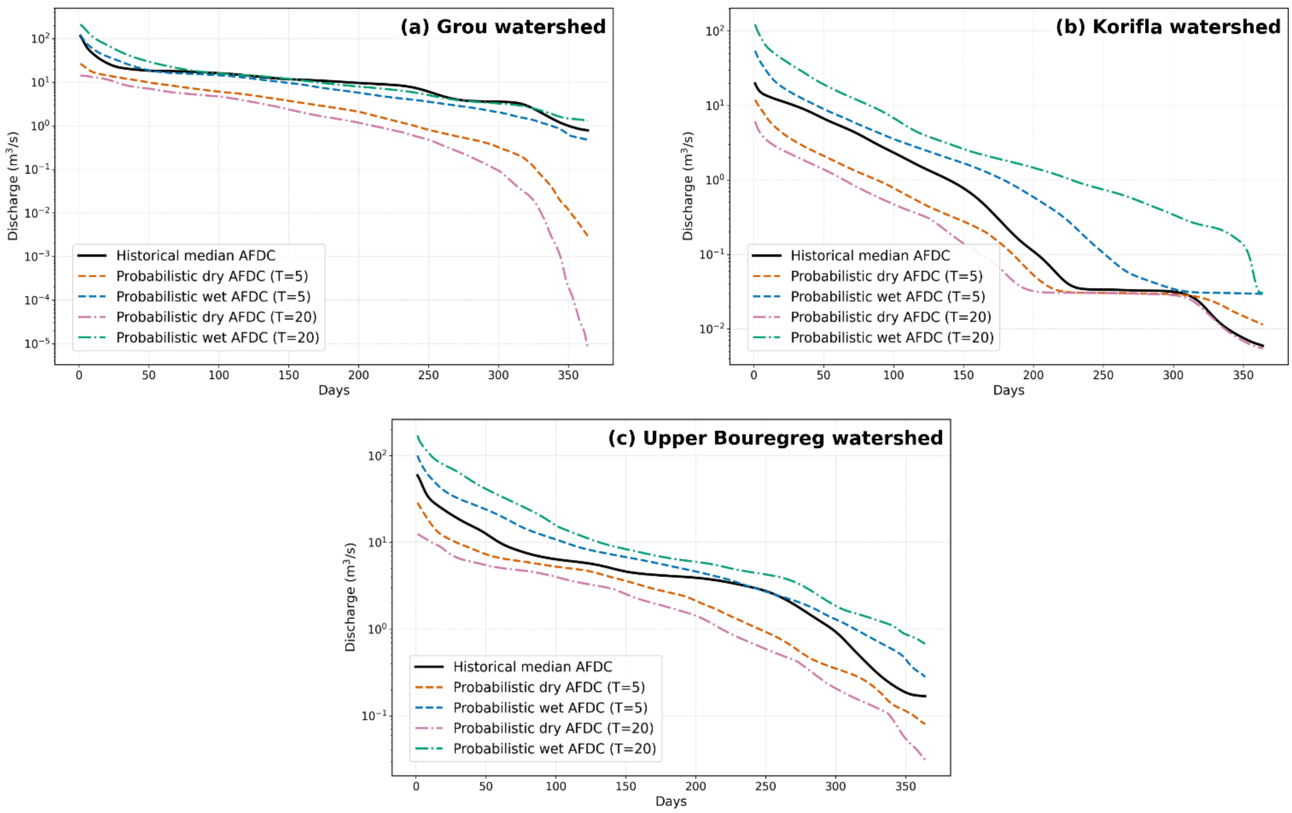

Fig. 6 Median and probabilistic AFDCs for 5-year and 20- year return periods at the outlets of the subwatersheds.

Table 4
NSE_{FDC} values for simulated AFDCs across the hydrological stations

Station	AE	LC	SA	TS	RF	SJ	OH	AL	SM
NSEFDC	0.53	0.6	0.57	0.6	0.5	0.54	0.35	0.65	0.51

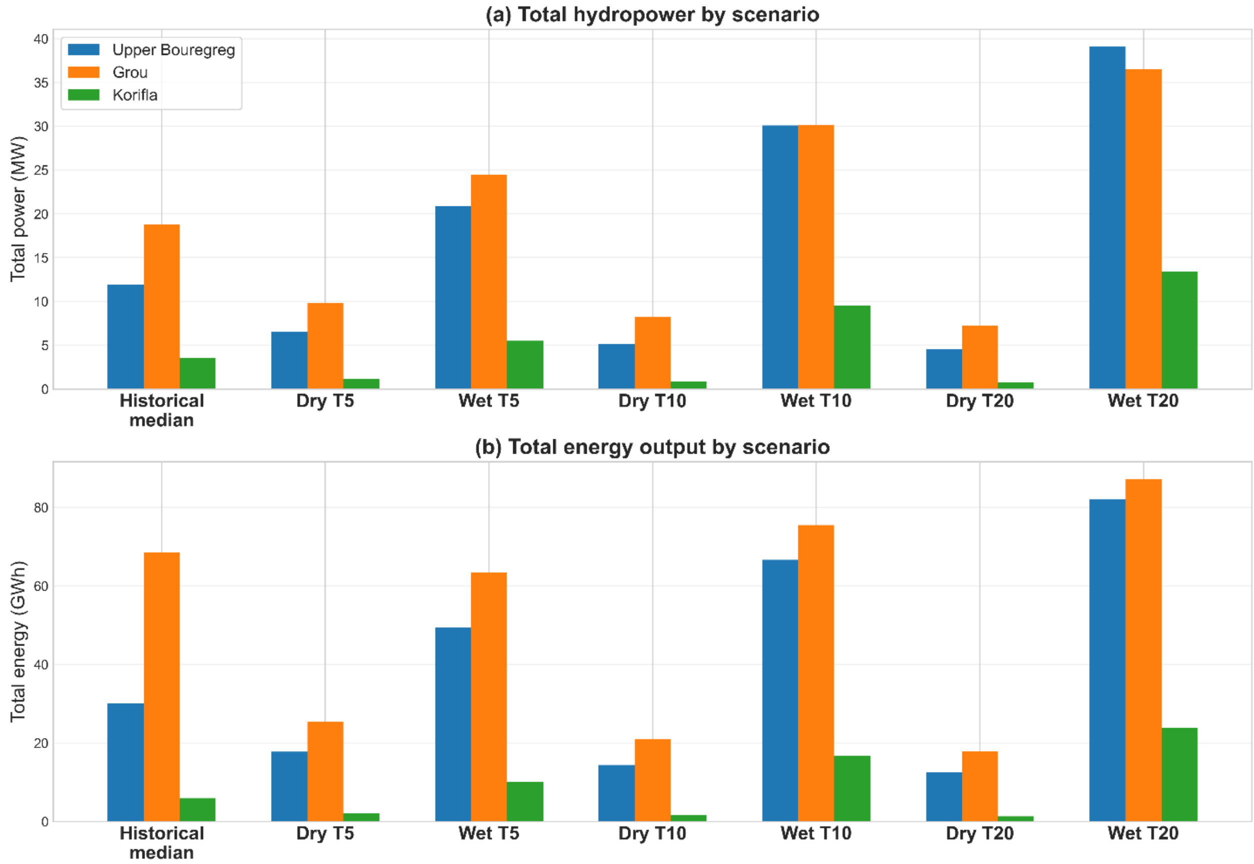

Fig. 7 Total hydropower potential and energy output under different hydrological scenarios across the subwatersheds: (a) total power and (b) total annual energy output.

Table 5
Technical hydropower potential, annual energy production, and population electricity demand coverage in the Bouregreg watershed under median, dry, and wet hydrological scenarios

Scenario	Historical median	Dry T5	Wet T5	Dry T10	Wet T10	Dry T20	Wet T20
Technical hydropower potential (MW)	34.3	17.6	50.8	14.3	69.7	12.5	89.0
Annual energy production (GWh/year)	104.7	45.3	122.9	37.0	158.7	31.8	193.0
Population electricity demand covered (%)	17.5	7.6	20.6	6.2	26.6	5.3	32.3

conditions, suggesting a more gradual distribution of low flows during wetter years.

3.3 Energy estimation of the RoR sites

Based on the adopted technical assumptions, the technical hydropower potential and annual energy output were estimated under the different hydrological conditions using the modular turbine configuration. The results obtained for each watershed are presented in Fig. 7, while the total technical potential and annual energy production are summarized in Table 5.

Although the installed capacity remains moderate under typical conditions, with a total of 34.3 MW, the corresponding annual energy production is relevant at the local scale. Based on the 2024 population density map and an average annual electricity consumption of 1219 kWh per person in Morocco, the proposed schemes could supply the annual electricity demand equivalent to approximately 17.5% of the population living within the Bouregreg watershed under typical hydrological conditions (Bondarenko *et al.*, 2025; Low Carbon Power, 2024). This share decreases gradually from one dry scenario to another, while the increase is more pronounced under progressively wetter scenarios, as presented in Table 5. This behavior suggests that the modular turbine configuration helps limit energy losses under dry conditions, while most of the additional energy gains occur during wet years. This aspect is discussed in more detail in the following section.

At the subwatershed scale, the Grou subwatershed provides overall the highest technical hydropower potential in most scenarios, followed closely by the Upper Bouregreg subwatershed, whereas Korifla remains substantially lower. According to Eq. 1, the hydropower potential is directly proportional to the design discharge. Therefore, the observed differences mainly reflect variations in the 30-day discharge extracted from the AFDCs. In terms of annual energy output, the Grou subwatershed also dominates in most scenarios. Unlike the hydropower potential, annual energy depends not only on the design discharge but also on the persistence of exploitable flows throughout the year, represented by the area under the PDC. The results therefore indicate that, in most cases, the Grou subwatershed maintains comparatively higher discharges over a large part of the year.

However, a higher technical hydropower potential does not necessarily lead to the highest annual energy production, since energy output depends on both the magnitude and the persistence of available flows. This distinction is illustrated by the Wet T20 scenario, where the Upper Bouregreg subwatershed with the highest potential does not necessarily produce the highest annual energy. In other words, two RoR sites may have the same design discharge and therefore the same hydropower potential, yet if one site exhibits a more variable flow regime, it may ultimately produce less energy over the year. A site with a more sustained flow regime and a flatter FDC may generate more energy than a site with a steeper or more variable flow regime. Therefore, for annual energy production, sites characterized by persistent medium flows and sustained discharge availability throughout the year are more favorable than sites with high but short-duration flows.

3.3.1 Performance of the modular turbine configuration

The proposed modular configuration considered a turbine number ranging from 2 to 10 turbines per RoR site. The results presented previously correspond to the configuration that maximized the annual energy output at each RoR site. For illustration, Fig. 8 presents the variation of annual energy production with the number of turbines for the RoR sites located at the outlets of the three watersheds, under three representative scenarios: the historical median, Wet T10, and Dry T10. The existence of an optimal number of turbines can be explained by the progressive subdivision of the design discharge in a modular configuration. As the number of turbines increases, the design discharge per unit decreases, and so does the minimum operating discharge of each turbine. This allows the last operating turbine to remain active over a longer portion of the low-flow tail of the PDC, thereby extending the exploitable flow range. However, increasing the number of turbines also introduces a larger number of operating thresholds. As discharge decreases, the modular plant undergoes more frequent transitions from *n* active turbines to *n-1,n-2,* and eventually one active turbine. In other words, the final plant shutdown is delayed, but intermediate unit shutdowns become more frequent. Beyond a certain number of turbines, the additional gain obtained from exploiting lower flows is no longer sufficient to compensate for the increased partial-load operation and the fragmentation of turbine activity. Consequently, annual energy production reaches a maximum and then decreases, defining an optimal modular configuration.

Fig. 9 presents the additional annual energy obtained when using the optimized modular configuration instead of a single turbine across the different watersheds and hydrological scenarios. A single turbine operates within a limited discharge range, bounded by a minimum operating discharge Q_{min} and a maximum admissible discharge Q_{max}. When several smaller turbines are installed in parallel, the minimum operating discharge of each unit is lower than that of an equivalent single large turbine, allowing the plant to exploit lower flows. Conversely, the maximum admissible discharge of a single turbine remains limited to Q_{max}, so part of the high-flow range cannot be fully exploited. In contrast, the modular configuration increases the plant-level admissible discharge to approximately nQ_{max}, where n is the number of turbines in operation.

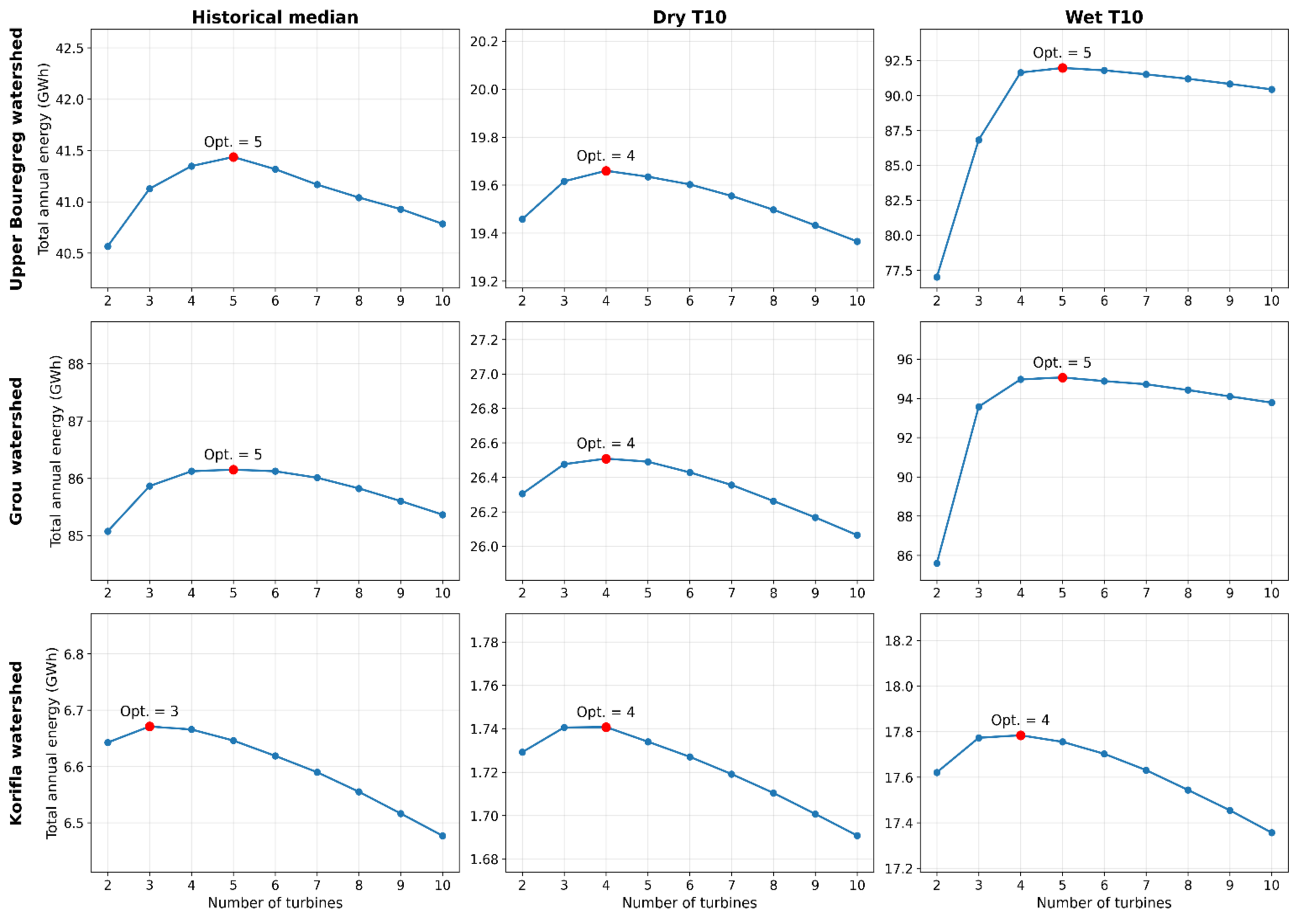

Fig. 8 Effect of the number of turbines on annual energy output in the modular configuration under historical median, Dry T10, and Wet T10 scenarios across the outlets of the subwatersheds.

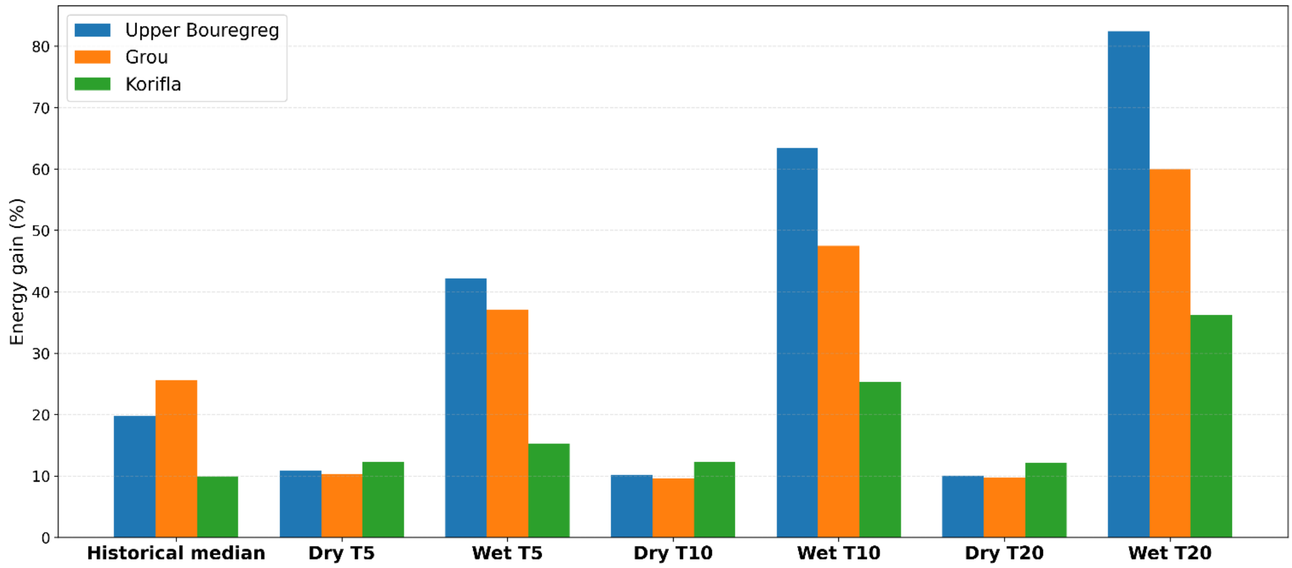

Fig. 9 Energy gain achieved by the modular turbine configuration compared with a single turbine configuration under different hydrological scenarios across the subwatersheds

Therefore, modular configurations tend to extend the exploitable range of the FDC, both toward lower and higher discharges.

For median hydrological conditions, the highest energy gain is observed in the Grou subwatershed, followed by the Upper Bouregreg subwatershed, while Korifla shows the lowest gain. This behavior can be partly explained by the shape of the AFDC. The effectiveness of modular turbines depends strongly on the steepness of the AFDC. In a steep AFDC, discharge decreases rapidly with exceedance duration, meaning that the additional low-flow range made available by modular turbines contributes only over a limited portion of the year. Conversely, in a flatter AFDC, low-to-medium flows persist over a longer duration, which increases the benefit of operating several smaller units. This explains why the gain is more pronounced in the Grou subwatershed, where the median AFDC is relatively less steep, and lower in Korifla, where the median AFDC shows a steeper decrease (Fig. 6)

The results also show that the energy gain increases under wetter hydrological scenarios, from Wet T5 to Wet T20. This increase is mainly related to the upper operating constraint of the single-turbine configuration. In each scenario, the plant design discharge is defined from the 30-day discharge. As hydrological conditions become wetter, the AFDC shifts upward, and design discharge increases accordingly. However, in the single-turbine configuration, the admissible flow remains bounded by the fixed maximum turbine capacity Q_{max}. Consequently, when the design discharge exceeds Q_{max}, the single turbine cannot exploit the full design discharge associated with the wet scenario. Instead, its production is increasingly capped by Q_{max}, leading to high-flow losses. In contrast, the modular configuration increases the plant-level admissible discharge to approximately nQ_{max}. Therefore, it can accommodate a larger part of the increased design discharge and exploit a wider portion of the high-flow range. This is reflected in the rapid increase in the energy gain from Wet T5 to Wet T20.

Under dry scenarios, the gain is more limited. As discharges decrease, the design discharge is less frequently constrained by the maximum turbine capacity. Consequently, the advantage of increasing the total admissible discharge through multiple turbines becomes less significant. In these conditions, the main benefit of modular operation is the ability to exploit lower flows, but the energy contribution of these flows remains relatively small. Therefore, the energy gain remains modest and varies only slightly between dry scenarios and watersheds. Overall, the results indicate that modular turbine configurations are particularly advantageous in watersheds with less steep AFDCs and under wetter hydrological conditions. Their main contribution is to enlarge the range of exploitable discharges, both by increasing the admissible high-flow capacity and by lowering the effective minimum operating threshold.

The results of the present study are consistent with previous RoR optimization studies, showing that the use of more than one turbine can improve energy production. Anagnostopoulos and Papantonis (2007) and Yildiz and Vrugt (2019) demonstrated that combining two turbines of different sizes can significantly enhance energy generation by expanding the range of exploitable discharges. More recently, Yildiz, Brown, and Rougé (2024) also considered multiple turbines with varying efficiencies in the optimization of RoR hydropower plants. However, configurations based on turbines of different sizes may increase operational complexity, particularly regarding flow allocation between units. They may also increase equipment and maintenance costs (Yildiz, Brown, & Rougé, 2024). For this reason, several optimization studies have considered multiple identical turbines operating in parallel. For example, Amougou *et al.* (2022) considered four similar turbines in the optimization of an existing RoR plant, while Kaldellis, Vlachou, and Korbakis (2005) assessed configurations ranging from one to three identical turbines in a techno-economic analysis of a new RoR plant. Similarly, Mamo *et al.* (2018) varied the number of identical turbines from one to five in a cost-optimization study. These studies show that the use of multiple identical turbines is a technically relevant and commonly adopted strategy for improving the balance between energy production, and operational simplicity in RoR hydropower plants. In this context, the present study extends the applicability of this solution to semi-arid watershed conditions and assesses the energy gain achieved by using a multi-turbine configuration instead of a conventional single-turbine RoR design in different hydrological conditions.

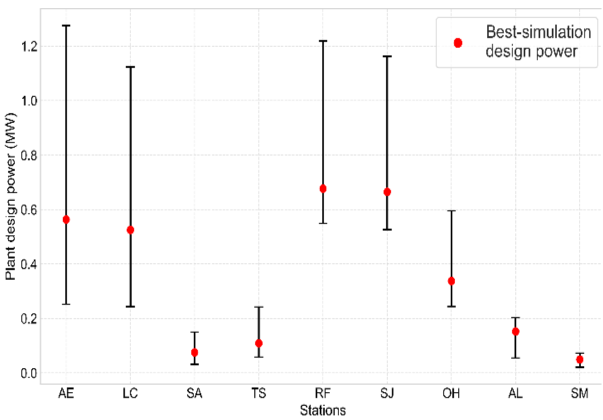

Fig. 10 Uncertainty bounds of plant design power at the gauging stations based on the 95PPU of simulated discharge.

3.3.2 Uncertainty bounds of hydropower potential estimates

By propagating uncertainty from the simulated discharge series to the hydropower potential calculations, lower and upper uncertainty bounds were obtained for each gauging station, as shown in Fig. 10.

The uncertainty width varies considerably across the basin, with the largest ranges observed at AE, LC, RF, and SJ. These disparities are not only related to the uncertainty in the SWAT-simulated discharges but also to the sensitivity of hydropower potential to discharge variations, as indicated by Eq. 1. Since plant design power is directly proportional to the design discharge, sites characterized by higher design discharges tend to show larger absolute variations in hydropower potential for a given discharge deviation. Consequently, stations characterized by higher design discharges, such as AE, LC, RF, and SJ, exhibit wider uncertainty intervals, whereas stations with lower design discharges, particularly in the Korifla subwatershed, show narrower ranges. Overall, the results indicate that uncertainty in the simulated AFDC can be amplified when propagated to plant design power, especially at sites where the selected design discharge is relatively high.

3.4 Economic performance and environmental considerations of the proposed RoR schemes

The preliminary economic assessment was carried out by estimating the capacity-weighted average LCOE for each watershed under median-year hydrological conditions. The results show clear differences between the three analysed watersheds. The average LCOE was estimated at 0.15 USD/kWh for the Upper Bouregreg subwatershed, 0.10 USD/kWh for the Grou subwatershed, and 0.18 USD/kWh for the Korifla subwatershed. The LCOE ranges obtained for individual RoR plants within each watershed are reported in Table 6. These results indicate that the Grou subwatershed presents the most favorable economic performance, followed by the Upper Bouregreg and Korifla subwatersheds. This ranking is consistent with the technical potential results, since watersheds with greater installed capacities tend to produce lower electricity costs (Klein & Fox, 2022).

Previous estimates for European small hydropower projects report LCOE values ranging approximately from 0.04 to 0.18 USD/kWh, while recent reports of global LCOE values for small hydropower, over the 2018–2024 period, ranged from about 0.051 to 0.102 USD/kWh (IRENA, 2012, 2025). In addition, long-term renewable energy cost projections have estimated an average small hydropower cost of around 0.108 USD/kWh by 2030 (Krewitt *et al.*, 2009). Within this context, the Grou subwatershed presents the most favorable economic performance, with values falling within the reported range for small hydropower projects. The Upper Bouregreg subwatershed is located in the upper, more expensive part of the benchmark ranges, whereas the Korifla subwatershed exceeds most of those values.

The relatively high costs obtained in this study are mainly explained by the proposed modular turbine configuration. Although modularity improves the exploitation of variable flows and increases annual energy recovery, it also increases the number of turbine-generator units, which represent a major share of RoR investment costs. Despite this cost penalty, the results remain encouraging for the most favourable watersheds. Nearly all plants in the Grou subwatershed and 70% of the plants in the Upper Bouregreg subwatershed present LCOE values lower than 0.15 USD/kWh, suggesting that these watersheds may contain economically promising sites for modular RoR development. In contrast, Korifla appears less economically attractive due to its lower estimated capacities and higher LCOE values.

When economic constraints are considered, the Grou subwatershed appears to be the most economically favorable among the studied watersheds. Therefore, if the development of the proposed RoR scheme were prioritized in the Grou subwatershed, the estimated annual energy production could supply the electricity demand equivalent to approximately 58% of its population under typical hydrological conditions. This result suggests that, despite the moderate scale of the proposed distributed RoR schemes, their contribution may be particularly relevant in watersheds where technical potential and economic feasibility are more closely aligned. Consequently, the Grou subwatershed could represent a priority area for further site-specific feasibility assessment and more detailed economic evaluation.

Beyond technical and economic feasibility, the development of multiple distributed RoR schemes along the same river network raises important environmental concerns, as the cumulative effects of successive low-head can be significant. Such projects can contribute to river fragmentation and affect physical, chemical, and biological processes, including flow continuity, sediment transport, water quality, and aquatic habitats (Sun *et al.*, 2025). For example, in the Mekong River

Table 6
Summary of LCOE values for the proposed RoR hydropower schemes in the three subwatersheds.

Subwatershed	Weighted average LCOE (USD/kWh)	Maximum site LCOE (USD/kWh)	Median site LCOE (USD/kWh)	Minimum site LCOE (USD/kWh)
Upper Bouregreg	0.150	0.205	0.149	0.079
Grou	0.105	0.178	0.099	0.053
Korifla	0.183	0.248	0.153	0.128

basin, the large number of dams, weirs, and sluice gates has been associated with severe habitat fragmentation and changes in fish distribution (Sun *et al.*, 2025). To reduce such impacts, the present study considered non-diversion RoR schemes, which are generally reported to have lower ecological impacts than diversion-type RoR plants (Kuriqi *et al.*, 2021). In addition, a minimum spacing criterion of 5 km between successive plants was imposed to limit the excessive concentration of barriers along the river network. Candidate sites located within protected areas were also excluded using the Protected Planet dataset to avoid proposing RoR sites in conservation areas, thereby further reducing the number of sites across the streams (UNEP-WCMC, 2026). An environmental flow constraint was also included in the potential estimation to maintain a minimum downstream flow regime, which is essential for sustaining aquatic habitats, water quality, sediment continuity, and river morphology (Kuriqi *et al.*, 2019). Such environmental flow requirements have been shown to reduce the ecological impacts of small hydropower plants (Kuriqi *et al.*, 2021). Overall, these measures do not eliminate the need for site-specific environmental assessment, but they provide a first-level screening framework to reduce the ecological risks associated with the spatial planning of distributed RoR schemes.

3.5 Limitations, future work, and study contribution

While the proposed framework estimates the technical hydropower potential of the studied watersheds, further refinements are still needed to support site-specific project development. The technical estimations were based on engineering assumptions, including the selected turbine type, design discharge, and weir height. Although these assumptions are suitable for a watershed-scale assessment, they should be refined in future feasibility studies at the project scale. The economic analysis should also be interpreted as an approximate cost estimation, given the sensitivity of RoR hydropower costs to local conditions.

Beyond the environmental constraints already considered in this study, the cumulative environmental effects of multiple distributed RoR schemes require further quantitative assessment. Future studies should evaluate these impacts at both river and watershed scales using indicators related to river fragmentation, flow alteration, habitat connectivity, and aquatic biodiversity (Jumani *et al.*, 2020; Lange *et al.*, 2018; Sun *et al.*, 2025). These ecological indicators could be integrated into a multi-objective optimization framework to identify alternative sites that minimize cumulative environmental impacts while maintaining acceptable energy production (Lange *et al.*, 2018). Finally, further sustainable potential assessments may incorporate public participation in decision-making processes related to RoR projects. Tools such as questionnaires and surveys can be used to evaluate local perceptions, concerns regarding land use, and potential impacts on livelihoods and quality of life (Rojanamon, Chaisomphob, & Bureekul, 2009).

Additionally, hydrological model performance can strongly influence hydropower calculations (Müller, Dralle, & Thompson, 2014). More generally, uncertainties in the simulated discharge series can propagate through the FDC to the design discharge. These deviations may then be amplified during hydropower calculations, because the design discharge affects not only the available flow itself, but also turbine sizing, efficiency estimation, the operating ranges of the modular turbine configuration, and consequently annual energy production. Therefore, for hydropower-oriented assessments, conventional calibration metrics should preferably be complemented by FDC-based indicators (Westerberg *et al.*, 2011).

Despite these limitations, the present study contributes to the assessment of RoR hydropower potential in Moroccan semi-arid watersheds. To the best of our knowledge, this study is among the first assessments of RoR hydropower in Morocco. A previous study focused on the Grou subwatershed and estimated the theoretical potential using three design-discharge scenarios, namely high-, medium-, and low-flow conditions (El Kasimi *et al.*, 2025). This method yielded a total theoretical potential of 32.4 MW in a median year when turbines from the three scenarios were considered side by side at each plant. In contrast, the present study expands the spatial scope to three semi-arid watersheds, namely Grou, Upper Bouregreg, and Korifla, and introduces a framework based on identical turbines operating in parallel. This framework also incorporates several technical and environmental constraints, including turbine type and number, operating configuration, turbine-generator efficiency, and environmental flows. These additions allowed the estimation of technical hydropower potential under multiple hydrological conditions, from a typical year to extremely dry and wet scenarios. In addition, a preliminary economic assessment was performed to provide an initial indication of the potential cost range of the proposed schemes and to compare their economic performance with values reported for existing small hydropower projects. Therefore, the novelty of the present work lies not only in the extension of the study area but also in the transition from theoretical potential mapping to an operationally constrained technical and preliminary economic assessment of RoR hydropower in a Moroccan semi-arid watershed.

4. Conclusion

Hydropower generation is strongly governed by the hydrological behavior of watersheds, which often limits its perceived feasibility in arid and semi-arid regions. Under such conditions, flow variability and low discharge availability can restrict the technical and economic attractiveness of RoR hydropower. Nevertheless, the results of this study suggest that, when appropriate technical configurations are considered, RoR hydropower may still represent a viable complementary renewable energy option in semi-arid basins.

Applied to the Bouregreg watershed in Morocco, the proposed framework combined hydrological modeling, a modular turbine configuration, and several technical and environmental constraints. Under normal hydrological conditions, the total technical hydropower potential was estimated at 34.3 MW. The assessment was further extended to extreme dry and wet conditions for return periods of 5, 10, and 20 years. The estimated potential decreased from 17.6 MW to 14.3 MW and 12.5 MW under increasingly dry conditions, while it increased from 50.8 MW to 69.7 MW and 89 MW under increasingly wet conditions. These results provide an indicative range of the probabilistic hydropower potential of the watershed and highlight the strong dependence of RoR production on hydrological variability.

In agreement with previous studies, the use of multiple turbines showed an energy production gain compared with a single-turbine configuration. This gain is mainly related to the extension of the admissible operating discharge range, both at low and high flows. The results also indicate that such a configuration is more advantageous at sites with relatively low interannual variability and during wetter hydrological conditions.

The preliminary cost assessment indicated that the proposed scheme would generally result in costs slightly higher than average values reported for small hydropower. However, some sites presented more favorable cost indicators, particularly within the Grou subwatershed, which also showed the highest technical potential across the assessed scenarios. If the scheme were developed only within this subwatershed, the estimated energy production under normal hydrological conditions could potentially supply approximately 58% of the annual electricity demand of its population.

The estimated potentials remain conditional on the technical and environmental assumptions adopted in this study, including the use of Crossflow turbines, the selected design discharge, the environmental flow constraint, and the fixed weir height. Therefore, the results should be interpreted as preliminary estimates of realistic RoR hydropower potential rather than final design values. Further site-specific investigations are needed to refine the assessment through detailed hydraulic, environmental, and economic analyses.

Nevertheless, the findings indicate that semi-arid watersheds, although often overlooked in hydropower development, may offer localized opportunities for decentralized renewable energy production. By integrating hydrological analysis, modular turbine design, and key technical and environmental constraints, the proposed framework can support early-stage planning and help identify sites where small-scale hydropower may complement broader sustainable energy strategies in water-limited regions.

Author Contributions: I. El Kasimi: Conceptualization, Data curation, Formal analysis, Methodology, Writing – original draft, Writing – review & editing; M.D. Hasnaoui: Conceptualization, Methodology, Resources, Validation, Writing – review & editing; D. Khomsi: Supervision, Validation, Writing – review & editing. All authors have read and agreed to the published version of the manuscript.

Funding: The authors received no financial support for the research, authorship, and/or publication of this article.

Conflicts of Interest: The authors declare no conflict of interest.

References

Abbaspour, K. C. (2015). SWAT-Calibration and Uncertainty Programs (CUP)—A User Manual. Swiss Federal Institute of Aquatic Science and Technology.

Adhikari, R., & Wood, D. (2018). The Design of High Efficiency Crossflow Hydro Turbines: A Review and Extension. Energies, 11(2), 267. https://doi.org/10.3390/en11020267

Agence du Bassin Hydraulique du Bouregreg et de la Chaouia. (n.d.). Infrastructure hydraulique. https://abhbc.com/fr/Bassin/infrastructure-hydraulique

AHEC. (2013). Project hydrology and installed capacity (Standards/Manuals/Guidelines for Small Hydro Development). Indian Institute of Technology Roorkee; Ministry of New and Renewable Energy, Government of India.

Ahmad, S., Mohsin Tahir, Asif Nawaz, Ghufran Ullah, Zeeshan Najam Khan, & Sheeraz Ahmed. (2024). Design and analysis of hydro turbines for electrical power generation. Kashf Journal of Multidisciplinary Research, 1(12), 153–168. https://doi.org/10.71146/kjmr162

Akinshin, A. (2024). Trimmed Harrell-Davis quantile estimator based on the highest density interval of the given width. Communications in Statistics - Simulation and Computation, 53(3), 1565–1575. https://doi.org/10.1080/03610918.2022.2050396

Amougou, C. B., Tsuanyo, D., Fioriti, D., Kenfack, J., Aziz, A., & Abiama, P. E. (2022). LCOE-Based Optimization for the Design of Small Run-of-River Hydropower Plants. Energies, 15(20). https://doi.org/10.3390/en15207507

Anagnostopoulos, J. S., & Papantonis, D. E. (2007). Optimal sizing of a run-of-river small hydropower plant. Energy Conversion and Management, 48(10), 2663–2670. https://doi.org/10.1016/j.enconman.2007.04.016

Arnold, J. G., Moriasi, D. N., Gassman, P. W., Abbaspour, K. C., White, M. J., Srinivasan, R., Santhi, C., Harmel, R. D., Griensven, A. V., Liew, M. W. V., Kannan, N., & Jha, M. K. (2012). SWAT: Model Use, Calibration, and Validation. Transactions of the ASABE, 55(4), 1491–1508. https://doi.org/10.13031/2013.42256

Arthington, A. H., Bhaduri, A., Bunn, S. E., Jackson, S. E., Tharme, R. E., Tickner, D., Young, B., Acreman, M., Baker, N., Capon, S., Horne, A. C., Kendy, E., McClain, M. E., Poff, N. L., Richter, B. D., & Ward, S. (2018). The Brisbane Declaration and Global Action Agenda on Environmental Flows (2018). Frontiers in Environmental Science, 6. https://doi.org/10.3389/fenvs.2018.00045

ASF DAAC. (2014). ALOS PALSAR High Resolution Radiometric Terrain Corrected Product. NASA Alaska Satellite Facility Distributed Active Archive Center. https://doi.org/10.5067/Z97HFCNKR6VA

Ayele, M. K. (2020). GIS Based Assessment of Hydropower Potential (A Case Study on Gumara River Basin). American Scientific Research Journal for Engineering, Technology, and Sciences, 69(1), 26–44. https://doi.org/https://asrjetsjournal.org/American_Scientific_Journal/article/view/5890

Bank of Canada. (n.d.). Currency converter. Bank of Canada. Retrieved June 8, 2026, from https://www.bankofcanada.ca/rates/exchange/currency-converter/

Basso, S., & Botter, G. (2012). Streamflow variability and optimal capacity of run-of-river hydropower plants. Water Resources Research, 48(10), 2012WR012017. https://doi.org/10.1029/2012WR012017

Biondi, D., Freni, G., Iacobellis, V., Mascaro, G., & Montanari, A. (2012). Validation of hydrological models: Conceptual basis, methodological approaches and a proposal for a code of practice. Physics and Chemistry of the Earth, Parts A/B/C, 42–44, 70–76. https://doi.org/10.1016/j.pce.2011.07.037

Bondarenko, M., Priyatikanto, R., Tejedor-Garavito, N., Zhang, W., McKeen, T., Cunningham, A., Woods, T., Cihan, D., Nosatiuk, B., Brinkhoff, T., Tatem, A., & Sorichetta, A. (2025). Constrained estimates of 2015–2030 total number of people per grid square at 3-arc resolution (approximately 100m at the equator) (Version v1) [Dataset]. WorldPop, University of Southampton.

Bragalli, C., Micocci, D., & Naldi, G. (2023). On the influence of net head and efficiency fluctuations over the performance of existing run-of-river hydropower plants. Renewable Energy, 206, 1170–1179. https://doi.org/10.1016/j.renene.2023.02.081

Bredeson, L., & Cicilio, P. (2023). Hydropower and Pumped Storage Hydropower Resource Review and Assessment for Alaska's Railbelt Transmission System. Energies, 16(14), 5494. https://doi.org/10.3390/en16145494

Castellarin, A., Galeati, G., Brandimarte, L., Montanari, A., & Brath, A. (2004). Regional flow-duration curves: Reliability for ungauged basins. Advances in Water Resources, 27(10), 953–965. https://doi.org/10.1016/j.advwatres.2004.08.005

Cherrad, B. (1997). Le bassin versant de l'oued Grou (plateau central marocain): Étude hydro-climatologique [Histoire, Université Paul Verlaine]. https://hal.science/tel-01777244/

Copernicus Climate Change Service. (2019). ERA5-Land hourly data from 1950 to present. Copernicus Climate Change Service (C3S) Climate Data Store (CDS). https://doi.org/10.24381/CDS.E2161BAC

Dhaubanjar, S., Lutz, A. F., Pradhananga, S., Smolenaars, W., Khanal, S., Biemans, H., Nepal, S., Ludwig, F., Shrestha, A. B., & Immerzeel, W. W. (2024). From theoretical to sustainable potential for run-of-river hydropower development in the upper Indus basin. Applied Energy, 357, 122372. https://doi.org/10.1016/j.apenergy.2023.122372

Duncan, N. (2012). Mapping Scotland's Hydropower Resource. The University of Edinburgh.

El Kasimi, I., Hasnaoui, M. D., Khomsi, D., Bouziane, A., & Aboulhassane, A. (2025). Optimal hydropower potential assessment in semi-arid regions. International Journal of Renewable Energy

Development, 14(5), 900–913. https://doi.org/10.61435/ijred.2025.60831
Ember. (2025). Global Electricity Mid-Year Insights 2025. In Ember. Ember. https://ember-energy.org/latest-insights/global-electricity-mid-year-insights-2025
Energy Sector Management Assistance Program. (2021). Assessing and Mapping Renewable Energy Resources. World Bank. https://www.esmap.org/node/57189
ESHA. (2004). Guide on how to develop a small hydropower plant. European Small Hydropower Association.
ESRI. (2013). World countries generalized [Dataset]. https://hub.arcgis.com/maps/esri::world-countries-generalized
Ezzaouini, M., Mahé, G., Kacimi, I., & Zerouali, A. (2020). Comparison of the MUSLE Model and Two Years of Solid Transport Measurement, in the Bouregreg Basin, and Impact on the Sedimentation in the Sidi Mohamed Ben Abdellah Reservoir, Morocco. Water, 12(7), 1882. https://doi.org/10.3390/w12071882
Fälth, H. E., Hedenus, F., Reichenberg, L., & Mattsson, N. (2025). Through energy droughts: Hydropower's ability to sustain a high output. Renewable and Sustainable Energy Reviews, 214, 115519. https://doi.org/10.1016/j.rser.2025.115519
FAO. (1971). FAO-UNESCO Soil Map of the World [Dataset]. https://www.fao.org/soils-portal/data-hub/soil-maps-and-databases/faounesco-soil-map-of-the-world/en/
Garcia, X., Estrada, L., Llorente, O., & Acuña, V. (2024). Assessing small hydropower viability in water-scarce regions: Environmental flow and climate change impacts using a SWAT+ based tool. Environmental Sciences Europe, 36(1), 126. https://doi.org/10.1186/s12302-024-00938-1
Gernaat, D. E. H. J., Bogaart, P. W., Vuuren, D. P. van, Biemans, H., & Niessink, R. (2017). High-resolution assessment of global technical and economic hydropower potential. Nature Energy, 2(10), 821–828. https://doi.org/10.1038/s41560-017-0006-y
Ghotbi, S., Wang, D., Singh, A., Blöschl, G., & Sivapalan, M. (2020). A New Framework for Exploring Process Controls of Flow Duration Curves. Water Resources Research, 56(1), e2019WR026083. https://doi.org/10.1029/2019WR026083
Golgojan, A.-D., White, C. J., & Bertram, D. (2025a). An assessment of run of river hydropower potential in Great Britain. Proceedings of the Institution of Civil Engineers - Water Management, 178(1), 42–61. https://doi.org/10.1680/jwama.23.00056
Hänggi, P., & Weingartner, R. (2012). Variations in Discharge Volumes for Hydropower Generation in Switzerland. Water Resources Management, 26(5), 1231–1252. https://doi.org/10.1007/s11269-011-9956-1
Harrell, F. E., & Davis, C. E. (1982). A new distribution-free quantile estimator. Biometrika, 69(3), 635–640. https://doi.org/10.1093/biomet/69.3.635
Hatata, A. Y., El-Saadawi, M. M., & Saad, S. (2019). A feasibility study of small hydro power for selected locations in Egypt. Energy Strategy Reviews, 24, 300–313. https://doi.org/10.1016/j.esr.2019.04.013
Hoes, O. A. C., Meijer, L. J. J., Van Der Ent, R. J., & Van De Giesen, N. C. (2017). Systematic high-resolution assessment of global hydropower potential. PLOS ONE, 12(2), e0171844. https://doi.org/10.1371/journal.pone.0171844
Huang, X., Hayashi, K., Fujii, M., Villa, F., Yamazaki, Y., & Okazawa, H. (2023). Identification of potential locations for small hydropower plant based on resources time footprint: A case study in Dan River Basin, China. Renewable Energy, 205, 293–304. https://doi.org/10.1016/j.renene.2023.01.079
IEA. (2020). Climate Impacts on African Hydropower. IEA. https://www.iea.org/reports/climate-impacts-on-african-hydropower
IEA. (2021). Hydropower Special Market Report. IEA. https://www.iea.org/reports/hydropower-special-market-report
IEA. (2025). Global Energy Review 2025. IEA. https://www.iea.org/reports/global-energy-review-2025
IHA. (2025). 2025 World Hydropower Outlook. IHA. https://www.hydropower.org/publications/2025-world-hydropower-outlook
International Finance Corporation. (2015). Hydroelectric Power: A guide for developers and investors. World Bank Group. https://openknowledge.worldbank.org/entities/publication/aaa516e4-e253-5c47-92c1-71c1c44ea2e4
IRENA. (2012). Renewable energy technologies: Cost analysis series.
IRENA. (2018). Global energy transformation: A roadmap to 2050. IRENA. https://www.irena.org/publications/2019/Apr/Global-energy-transformation-A-roadmap-to-2050-2019Edition
IRENA. (2025). Renewable power generation costs in 2024. IRENA. https://www.irena.org/Publications/2025/Jun/Renewable-Power-Generation-Costs-in-2024
Joshi, T. P., & Mishra, B. K. (2024). Assessment of Run-of-River Hydropower Potential Using SWAT Modeling and GIS in the Marsyangdi River Basin, Nepal. Journal of Hydrology and Meteorology, 12(1), 11–22. https://doi.org/10.3126/jhm.v12i1.72651
Jumani, S., Deitch, M. J., Kaplan, D., Anderson, E. P., Krishnaswamy, J., Lecours, V., & Whiles, M. R. (2020). River fragmentation and flow alteration metrics: A review of methods and directions for future research. Environmental Research Letters, 15(12), 123009. https://doi.org/10.1088/1748-9326/abcb37
Kadier, A., Kalil, M. S., Pudukudy, M., Hasan, H. A., Mohamed, A., & Hamid, A. A. (2018). Pico hydropower (PHP) development in Malaysia: Potential, present status, barriers and future perspectives. Renewable and Sustainable Energy Reviews, 81, 2796–2805. https://doi.org/10.1016/j.rser.2017.06.084
Kaldellis, J. K., Vlachou, D. S., & Korbakis, G. (2005). Techno-economic evaluation of small hydro power plants in Greece: A complete sensitivity analysis. Energy Policy, 33(15), 1969–1985. https://doi.org/10.1016/j.enpol.2004.03.018
Karra, K., Kontgis, C., Statman-Weil, Z., Mazzariello, J. C., Mathis, M., & Brumby, S. P. (2021). Global land use / land cover with Sentinel 2 and deep learning. 2021 IEEE International Geoscience and Remote Sensing Symposium IGARSS, 4704–4707. https://doi.org/10.1109/IGARSS47720.2021.9553499
Khaleghi, M. R., & Hosseini, S. H. (2024). Using SWAT and SWAT-CUP for hydrological simulation and uncertainty analysis of the arid and semiarid watersheds (Case study: Zoshk Watershed, Shandiz, Iran). Applied Water Science, 14(12), 266. https://doi.org/10.1007/s13201-024-02327-8
Khan, F. A., & Pal, N. (2020). Hydropower technology. In Sustainable Fuel Technologies Handbook (1st ed., pp. 91–118). Academic Press.
Killingtveit, Å. (2020). Hydroelectric Power. In Future Energy (pp. 315–330). Elsevier. https://doi.org/10.1016/B978-0-08-102886-5.00015-3
Kim, K. B., Kwon, H.-H., & Han, D. (2018). Exploration of warm-up period in conceptual hydrological modelling. Journal of Hydrology, 556, 194–210. https://doi.org/10.1016/j.jhydrol.2017.11.015
Klein, S. J. W., & Fox, E. L. B. (2022). A review of small hydropower performance and cost. Renewable and Sustainable Energy Reviews, 169, 112898. https://doi.org/10.1016/j.rser.2022.112898
Krewitt, W., Nienhaus, K., Kleßmann, C., Capone, C., Stricker, E., Graus, W., Hoogwijk, M., Supersberger, N., von Winterfeld, U., & Samadi, S. (2009). Role and Potential of Renewable Energy and Energy Efficiency for Global Energy Supply. Umweltbundesamt. https://www.umweltbundesamt.de/en/publikationen/role-potential-of-renewable-energy-energy
Kumar, A., Schei, T., Ahenkorah, A., Caceres Rodriguez, R., Devernay, J.-M., Freitas, M., Hall, D., Killingtveit, Å., & Liu, A. (2011). Hydropower. In IPCC Special Report on Renewable Energy Sources and Climate Change Mitigation (pp. 437–496). Cambridge University Press.
Kuriqi, A., Pinheiro, A. N., Sordo-Ward, A., Bejarano, M. D., & Garrote, L. (2021). Ecological impacts of run-of-river hydropower plants—Current status and future prospects on the brink of energy transition. Renewable and Sustainable Energy Reviews, 142, 110833. https://doi.org/10.1016/j.rser.2021.110833
Kuriqi, A., Pinheiro, A. N., Sordo-Ward, A., & Garrote, L. (2019). Influence of hydrologically based environmental flow methods on flow alteration and energy production in a run-of-river hydropower plant. Journal of Cleaner Production, 232, 1028–1042. https://doi.org/10.1016/j.jclepro.2019.05.358
Kusre, B. C., Baruah, D. C., Bordoloi, P. K., & Patra, S. C. (2010). Assessment of hydropower potential using GIS and hydrological modeling technique in Kopili River basin in Assam (India). Applied Energy, 87(1), 298–309. https://doi.org/10.1016/j.apenergy.2009.07.019

Lange, K., Meier, P., Trautwein, C., Schmid, M., Robinson, C. T., Weber, C., & Brodersen, J. (2018). Basin-scale effects of small hydropower on biodiversity dynamics. Frontiers in Ecology and the Environment, 16(7), 397–404. https://doi.org/10.1002/fee.1823
Li, C. Z., Zhang, L., Wang, H., Zhang, Y. Q., Yu, F. L., & Yan, D. H. (2012). The transferability of hydrological models under nonstationary climatic conditions. Hydrology and Earth System Sciences, 16(4), 1239–1254. https://doi.org/10.5194/hess-16-1239-2012
Low Carbon Power. (2024). Electricity in Morocco in 2024. https://lowcarbonpower.org/region/Morocco
Magaju, D., Cattapan, A., & Franca, M. (2020). Identification of run-of-river hydropower investments in data scarce regions using global data. Energy for Sustainable Development, 58, 30–41. https://doi.org/10.1016/j.esd.2020.07.001
Malhan, P., & Mittal, M. (2021). Evaluation of different statistical techniques for developing cost correlations of micro hydro power plants. Sustainable Energy Technologies and Assessments, 43, 100904. https://doi.org/10.1016/j.seta.2020.100904
Mamo, G., Marence, M., Chacon-Hurtado, J., & Franca, M. (2018). Optimization of Run-of-River Hydropower Plant Capacity. International Water Power and Dam Construction. https://www.researchgate.net/publication/326942666_Optimization_of_Run-of-River_Hydropower_Plant_Capacity
Marcinkowski, P. (2025). Large-scale assessment of hydropower potential: Current state and future projections for Poland. Energy, 328, 136700. https://doi.org/10.1016/j.energy.2025.136700
Maroufpoor, S., & Qin, X. (2025). Present and Future Energy Potential of Run-of-River Hydropower in Mainland Southeast Asia: Balancing Climate Change and Environmental Sustainability. Water, 17(15), 2256. https://doi.org/10.3390/w17152256
Martins Da Silva, F. W., Camacho, J. R., & Ferreira, J. H. I. (2024). Analysis of hydraulic losses in the series from 1990 to 2022 at the Retiro small hydroelectric power plant. Heliyon, 10(8), e29627. https://doi.org/10.1016/j.heliyon.2024.e29627
Mehr, G., Durali, M., Khakrand, M. H., & Hoghooghi, H. (2021). A novel design and performance optimization methodology for hydraulic Cross-Flow turbines using successive numerical simulations. Renewable Energy, 169, 1402–1421. https://doi.org/10.1016/j.renene.2021.01.090
Mills-Novoa, M., & Borgias, S. (2025). The new era of contested hydropower development: A systematic review from 2000 to 2022. World Development, 196, 107162. https://doi.org/10.1016/j.worlddev.2025.107162
Minister of Natural Resources Canada. (2004). Small hydro project analysis. In Clean Energy Project Analysis: RETScreen Engineering & Cases Textbook. RETScreen International.
Moriasi, D. N., Gitau, M. W., Daggupati, P., & Pai, N. (2015). Hydrologic and Water Quality Models: Performance Measures and Evaluation Criteria. Transactions of the ASABE, 58(6), 1763–1785. https://doi.org/10.13031/trans.58.10715
Müller, M. F., Dralle, D. N., & Thompson, S. E. (2014). Analytical model for flow duration curves in seasonally dry climates. Water Resources Research, 50(7), 5510–5531. https://doi.org/10.1002/2014WR015301
Naidu, S., Chand, A., Pandaram, A., & Vosikata, S. (2024). Electricity Consumption, Renewable Energy Production, and Current Account of Organisation for Economic Co-Operation and Development Countries: Implications for Sustainability. Sustainability, 16(9), 3722. https://doi.org/10.3390/su16093722
Nandnaba, A. M. (2025). The dark political side of US economic sanctions: An overview of renewable energy production in developing countries. Energy, 335, 138062. https://doi.org/10.1016/j.energy.2025.138062
Pandey, A., Lalrempuia, D., & Jain, S. K. (2015). Assessment of hydropower potential using spatial technology and SWAT modelling in the Mat River, southern Mizoram, India. Hydrological Sciences Journal, 60(10), 1651–1665. https://doi.org/10.1080/02626667.2014.943669
Pandey, B., & Karki, A. (2016). Hydroelectric Energy. CRC Press. https://doi.org/10.1201/9781315374840
Paschetto, A., Caselle, C., & Bonetto, S. M. R. (2025). A GIS-based methodology for hydropower potential assessment: Balancing energy production and ecosystem sustainability. Environmental Challenges, 20, 101236. https://doi.org/10.1016/j.envc.2025.101236
Penche, C. (1998). Layman's Guidebook on How to Develop Small Hydro Site. ESHA.
Ridolfi, E., Kumar, H., & Bárdossy, A. (2020). A methodology to estimate flow duration curves at partially ungauged basins. Hydrology and Earth System Sciences, 24(4), 2043–2060. https://doi.org/10.5194/hess-24-2043-2020
Rojanamon, P., Chaisomphob, T., & Bureekul, T. (2009). Application of geographical information system to site selection of small run-of-river hydropower project by considering engineering/economic/environmental criteria and social impact. Renewable and Sustainable Energy Reviews, 13(9), 2336–2348. https://doi.org/10.1016/j.rser.2009.07.003
Roy, N., Sutradhar, R., Mandal, S., Sarma, R., & Debnath, K. (2022). Operational and Economic challenges due to Run-of-River (RoR) Hydro and ways to address the challenges. 2022 4th International Conference on Energy, Power and Environment (ICEPE), 1–6. https://doi.org/10.1109/ICEPE55035.2022.9798383
Rumbayan, M., & Rumbayan, R. (2023). Feasibility Study of a Micro Hydro Power Plant for Rural Electrification in Lalumpe Village, North Sulawesi, Indonesia. Sustainability, 15(19), 14285. https://doi.org/10.3390/su151914285
Sahrakorpi, T., Khosravi, A., & Assad, M. E. H. (2021). Hydropower. In Design and Performance Optimization of Renewable Energy Systems (pp. 181–194). Elsevier. https://doi.org/10.1016/B978-0-12-821602-6.00014-6
Sasthav, C., & Oladosu, G. (2022). Environmental design of low-head run-of-river hydropower in the United States: A review of facility design models. Renewable and Sustainable Energy Reviews, 160, 112312. https://doi.org/10.1016/j.rser.2022.112312
Schroeder, R., Loots, I., Van Dijk, M., & Coetzee, G. l. (2023). Development of a procedure and tool for retrofit hydropower evaluation at South African dams. Water SA, 49(3 July). https://doi.org/10.17159/wsa/2023.v49.i3.3980
Shen, H., Tolson, B. A., & Mai, J. (2022). Time to Update the Split-Sample Approach in Hydrological Model Calibration. Water Resources Research, 58(3), e2021WR031523. https://doi.org/10.1029/2021WR031523
Singal, S. K., Saini, R. P., & Raghuvanshi, C. S. (2010). Analysis for cost estimation of low head run-of-river small hydropower schemes. Energy for Sustainable Development, 14(2), 117–126. https://doi.org/10.1016/j.esd.2010.04.001
Sun, J., Baldan, D., Lucas, M. C., Wang, J., Rodeles, A. A., Galib, S. M., Tao, J., Li, M., He, D., & Ding, C. (2025). Widespread and strong impacts of river fragmentation by anthropogenic barriers on fishes in the Mekong River Basin. Communications Earth & Environment, 6(1), 534. https://doi.org/10.1038/s43247-025-02467-y
Tefera, W. M., & Kasiviswanathan, K. S. (2022). A global-scale hydropower potential assessment and feasibility evaluations. Water Resources and Economics, 38, 100198. https://doi.org/10.1016/j.wre.2022.100198
Thin, K. K., Zin, W. W., San, Z. M. L. T., Kawasaki, A., Moiz, A., Bhagabati, S. S. (2020). Estimation of Run-of-River Hydropower Potential in the Myitnge River Basin. Journal of Disaster Research, 15(3), 267–276. https://doi.org/10.20965/jdr.2020.p0267
Tsuanyo, D., Amougou, B., Aziz, A., Nka Nnomo, B., Fioriti, D., & Kenfack, J. (2023). Design models for small run-of-river hydropower plants: A review. Sustainable Energy Research, 10(1), 3. https://doi.org/10.1186/s40807-023-00072-1
UNEP-WCMC. (2026). Protected Area Profile for Morocco from the World Database on Protected Areas [Map]. www.protectedplanet.net
UNIDO & ICSHP. (2022). World Small Hydropower Development Report 2022. United Nations Industrial Development Organization, International Center on Small Hydro Power. . https://www.unido.org/WSHPDR2022
U.S. Department of Energy. (n.d.). Microhydropower Systems. https://www.energy.gov/energysaver/microhydropower-systems
Verán-Leigh, D., & Vázquez-Rowe, I. (2019). Life cycle assessment of run-of-river hydropower plants in the Peruvian Andes: A policy support perspective. International Journal of Life Cycle Assessment, 24(8), 1376–1395. https://doi.org/10.1007/s11367-018-01579-2

Vogel, R. M., & Fennessey, N. M. (1994). Flow-Duration Curves. I: New Interpretation and Confidence Intervals. Journal of Water Resources Planning and Management, 120(4), 485–504. https://doi.org/10.1061/(ASCE)0733-9496(1994)120:4(485)

Wagner, H.-J., & Mathur, J. (2011). Economics of Hydropower Plants. In H.-J. Wagner & J. Mathur (Eds.), Introduction to Hydro Energy Systems: Basics, Technology and Operation (pp. 111–117). Springer. https://doi.org/10.1007/978-3-642-20709-9_7

Westerberg, I. K., Guerrero, J.-L., Younger, P. M., Beven, K. J., Seibert, J., Halldin, S., Freer, J. E., & Xu, C.-Y. (2011). Calibration of hydrological models using flow-duration curves. Hydrology and Earth System Sciences, 15(7), 2205–2227. https://doi.org/10.5194/hess-15-2205-2011

Wheater, H. (2025). Why is arid zone hydrology a scientific desert—And how does the hydrological community move forward? Environmental Modelling & Software, 192, 106561. https://doi.org/10.1016/j.envsoft.2025.106561

Wu, H., & Chen, B. (2015). Evaluating uncertainty estimates in distributed hydrological modeling for the Wenjing River watershed in China by GLUE, SUFI-2, and ParaSol methods. Ecological Engineering, 76, 110–121. https://doi.org/10.1016/j.ecoleng.2014.05.014

Yildiz, V., Brown, S., & Rougé, C. (2024). Importance of Variable Turbine Efficiency in Run-Of-River Hydropower Design Under Deep Uncertainty. Water Resources Research, 60(6), e2023WR035713. https://doi.org/10.1029/2023WR035713

Yildiz, V., & Vrugt, J. A. (2019). A toolbox for the optimal design of run-of-river hydropower plants. Environmental Modelling & Software, 111, 134–152. https://doi.org/10.1016/j.envsoft.2018.08.018